

Review

Activation of C₂–C₄ alkanes over acid and bifunctional zeolite catalysts

G. Caeiro^a, R.H. Carvalho^a, X. Wang^a, M.A.N.D.A. Lemos^a,
F. Lemos^a, M. Guisnet^{a,b,*}, F. Ramôa Ribeiro^a

^a Centro de Engenharia Biológica e Química, Instituto Superior Técnico, Av. Rovisco Pais, 1049-001 Lisboa, Portugal

^b Laboratoire de Catalyse en Chimie Organique (UMR 6503), Université de Poitiers, 40 Avenue du Recteur Pineau, 86022 Poitiers, France

Received 27 February 2006; accepted 30 March 2006

Available online 12 May 2006

Abstract

This review paper presents the significant advances which were made in the last decade in the understanding of the transformation over acid and bifunctional zeolite catalysts of the cheap and readily available C₂–C₄ alkanes into more valuable products: mechanism of activation, reaction scheme, nature of the active sites. Both the transformations of pure alkanes: *n*-butane isomerization, C₂–C₄ alkane aromatization and of alkanes in mixture with alkenes: isobutane–butene alkylation or with aromatic hydrocarbons: benzene alkylation with ethane or propane are considered.

© 2006 Elsevier B.V. All rights reserved.

Keywords: C₂–C₄ alkanes; Activation; Aromatization; Butane isomerization; Dehydroisomerization; Isobutane–butene alkylation; Benzene alkylation; Mechanism; Zeolite catalysts

Contents

1. Introduction	132
2. Transformation of light alkanes over acid zeolites	132
2.1. Activation mechanisms	132
2.1.1. The carbenium-chain mechanism	132
2.1.2. The protolytic mechanism	133
2.1.3. Conclusion	134
2.2. Disproportionation and isomerization	135
2.2.1. Reaction mechanism	135
2.2.2. Influence of the acidity and pore structure of the zeolite catalysts	138
2.2.3. Conclusion	138
2.3. Light alkanes aromatization	138
2.3.1. Reaction scheme	139
2.3.2. Conclusion	140
2.4. Alkylation of isobutane with <i>n</i> -butene	140
2.4.1. Chemistry of alkylation	140
2.4.2. How to limit deactivation?	140
2.4.3. Novel regeneration methods	142
2.4.4. Conclusion	142
3. Transformation of light alkanes over metal zeolite catalysts	142
3.1. Main features of light alkane aromatization	143
3.1.1. Demonstration (and nature) of a bifunctional aromatization scheme	143
3.1.2. Other reactions involved in propane transformation over Ga/HMFI catalysts	144

* Corresponding author.

E-mail address: michel.guisnet@univ-poitiers.fr (M. Guisnet).

3.1.3.	Dehydrogenation steps. A bifunctional mechanism?	145
3.1.4.	Composition of the working catalyst	147
3.1.5.	Comparison of Zn and of Ga/MFI catalysts	148
3.1.6.	Conclusion	149
3.2.	<i>n</i> -Butane hydroisomerization and dehydroisomerization	149
3.2.1.	Hydroisomerization of <i>n</i> -butane	149
3.2.2.	Dehydroisomerization of <i>n</i> -butane	150
3.3.	Alkylation of aromatics with small alkanes	152
3.3.1.	Thermodynamic considerations	152
3.3.2.	Alkylation over Pt or Pd/HMFI catalysts	153
3.3.3.	Alkylation over Ga/HMFI catalysts	154
3.3.4.	Conclusion	155
4.	General conclusion	155
	Acknowledgements	155
	References	155

1. Introduction

The activation of short-chain alkanes is one of the great challenges of the present catalysis research. Indeed, the direct use of these cheap and readily available materials will provide an attractive alternative to the processes that are currently based on alkenes and aromatics [1,2]. The objective of this paper is to present the recent advances in the field of C₂–C₄ alkanes non-oxidative activation and transformation into valuable products over zeolite catalysts.

C₂–C₄ alkanes are often associated with methane in natural gas and are also formed in significant amounts in catalytic cracking (FCC). Ethane and propane can be used as refinery fuel, propane as liquefied petroleum gas (LPG) alone or in mixture with butane. C₂–C₄ alkanes can be used as feedstock in steam cracking for the production of short-chain alkenes and of benzenic hydrocarbons. Aromatization over Ga/MFI catalysts constitutes another alternative for the valorization of C₃–C₄ alkanes [3–7]. Butanes can be used as components of gasoline or as feedstock to various refinery processes. *n*-Butane can be isomerized into isobutane [7,8]. A large part of isobutane is used in alkylation units for the production of high octane C₈ branched alkanes, another one is dehydrogenated into isobutene for the production of methyl tertio butyl ether (MTBE) [8].

Most of these processes involve acid or bifunctional metal acid catalysts. Zeolite catalysts are already used in aromatization processes [3–7] and could be used in isobutane–butene alkylation. Moreover, they are able to catalyze *n*-butane isomerization, even if their activity is too low in comparison to that of chlorinated alumina catalyst which is currently used [8]. Lastly zeolites are promising components of catalysts for more environment-friendly processes: oxydehydrogenation of propane [9–11], one pot bi-step transformations such as the production of isobutene by dehydroisomerization of *n*-butane [12] or the alkylation of benzene with ethane [13] or with propane [14].

The acid catalyzed reactions over zeolites will be presented in Section 2. Pure C₂–C₄ alkanes can only be transformed at

relatively high temperatures (>150 °C). Moreover, the reaction temperature determines the nature of their transformation:

- Disproportionation (and isomerization in the case of butanes) above 150 °C.
- Dehydrogenation, cracking and aromatization above 300 °C.

At temperatures lower than 150 °C, no reaction of pure alkanes can be observed. However, transformations appear when short-chain alkanes are used in mixture with alkenes (isobutane–butenes alkylation).

Section 3 deals with bifunctional catalysis transformations. The association of dehydrogenating species to the acid zeolites allows easier or/and more selective transformations of short-chain alkanes: aromatization over Ga/HMFI, isomerization and dehydroisomerization of *n*-butane over Pt or Pd/H zeolites, alkylation of benzene with ethane or propane over Pt or Ga/HMFI.

2. Transformation of light alkanes over acid zeolites

2.1. Activation mechanisms

2.1.1. The carbenium-chain mechanism

Until 20 years ago, it was widely accepted that the transformation of hydrocarbons over acid zeolites proceeded through a chain mechanism where carbenium ions acted as chain carriers [8]. Carbenium ions may undergo several reactions: deprotonation, hydride transfer, isomerization, β-scission (and oligomerization which is the reverse reaction). In alkane cracking, hydride transfer is the propagation step (Fig. 1), reason for which the cracking mechanism is commonly denominated as bimolecular. The stability of the carbenium ions increases with their degree of substitution: tertiary III > secondary II > primary I > methyl and the higher the stability of the carbenium ions involved in β-scission, the faster the step [15].

More recently, Kazansky and Senchenya [16] proposed that the real intermediates were not carbenium ions but covalent alkoxide species (Fig. 2). Contrarily to carbenium ions, there are little differences in stability between primary, secondary and

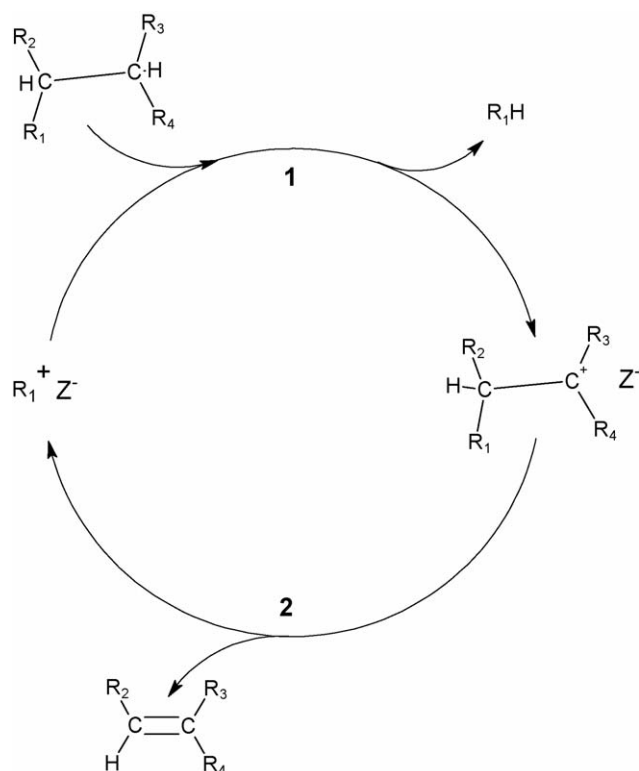


Fig. 1. Cracking of an alkane molecule through the carbenium ion-chain mechanism. Step 1: hydride transfer, Step 2: β -scission.

tertiary alkoxides. These results, based on ab initio quantum calculations with cluster models of zeolite were confirmed by other research groups [17–23]. Transition states are energetically excited ion pairs obtained by elongation of the alkoxides C–O bonds, the alkyl pairs resembling carbenium ions in geometry and charge (highly positive). This explains why the classical carbenium ion theory, although formally not exact, succeeds in explaining the cracking product distribution.

It should however be underscored that the local geometry of the zeolite acid sites can strongly influence the geometry and stability of alkoxide intermediates and in certain cases stabilize

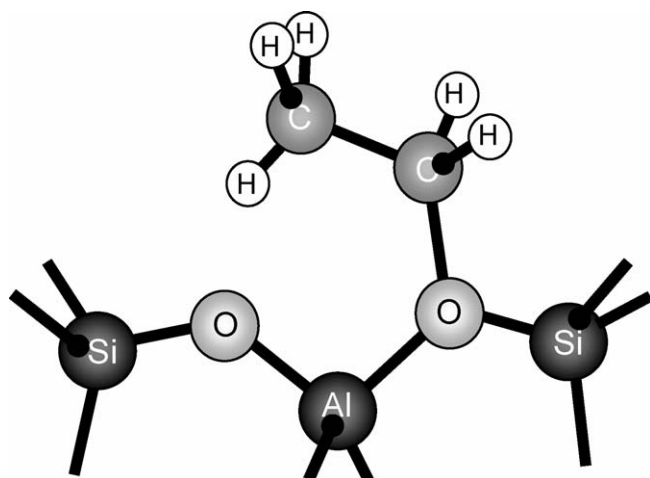


Fig. 2. Covalently bonded ethoxy group. Adapted from [20].

the ionic transition states, which could make possible reactions expected as very slow on the stability of the carbenium ion transition states. It could be why [24,25] the selective skeletal *n*-butene isomerization over HFER and HTON would occur through a monomolecular mechanism which in principle involves very unstable primary carbenium ions as transition states.

There are several ways to explain the initiation step (i.e., the formation of the first alkoxides) of alkane cracking over acidic zeolites [8,26]. Firstly, there can be alkene impurities in the feed which are much keener towards the interaction with acid sites than alkanes. It is important to point out that alkenes can also be produced by thermal cracking. Secondly, zeolites are not pure Brønsted acid catalysts. Varying with the zeolite, there are small or large amounts of extraframework aluminium species dispersed within the micropores or on the external surface and also framework defects. These species which are generally Lewis acid sites could activate alkanes. Lastly, according to Haag and Dessau [27], alkanes can also be transformed into olefins (and to other products: hydrogen or alkanes) on the zeolite Brønsted acid sites (protolytic dehydrogenation or cracking). Over certain zeolites and under chosen operating conditions, in particular at high temperatures ($>500^\circ\text{C}$) and low conversions, the products resulting from this transformation can be observed in large amounts, whereas at low temperatures and high conversions, they serve only for the initiation of the carbenium ion-chain mechanism.

2.1.2. The protolytic mechanism

The Haag and Dessau mechanism [27] based on Olah's superacid chemistry [28] is a monomolecular mechanism. According to this mechanism, zeolites protonate alkanes at high temperatures to give unstable transition states known as carbonium ions. These carbonium ions can easily collapse (Fig. 3) to produce H_2 (step 1) or small alkanes (step 2): methane, ethane, etc. plus carbenium ions (or rather the already mentioned alkoxides). The elected route, protolytic cracking or dehydrogenation, will depend if the proton attacks a C–C bond or a C–H bond of the reacting alkane.

Table 1 shows that in the transformation of C_2 – C_4 alkanes over HMF1 at 500°C , all the products expected from this mechanism are formed as primary products [29–32]. The reactivity of alkanes can also be explained through this mechanism: butanes are 4-times more reactive than propane and 100-times more than ethane. Moreover, a reaction order of one was found at low partial pressure of reactant in agreement with this monomolecular reaction.

In comparison with the carbenium ion-chain mechanism, protolysis is favored at high reaction temperatures, small partial pressures of alkane and low conversions [27]. These features can be related respectively with the higher activation energy (carbonium ions are more unstable than carbenium ion transition states), the monomolecular nature of protolysis and the fact that alkenes resulting from protolysis act as initiators of the chain mechanism.

In which regards the zeolite properties, the relevant factors are the size of the channels and cages and the strength and density of the acid protonic sites. Indeed, because of steric con-

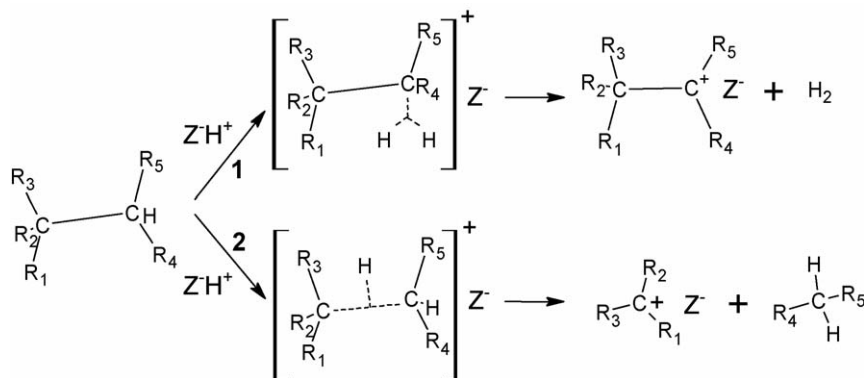


Fig. 3. Protolytic cracking and dehydrogenation of alkanes heavier than methane.

straints on the formation of the bimolecular transition states of the chain mechanism, the relative significance of this mechanism decreases with the size of the space available at the vicinity of the acid sites, hence protolysis appears as favored over narrow pores zeolites [27,33–35]. Furthermore, the more energetically demanding protolysis mechanism requires very strong protonic sites, such as those resulting from interaction of bridging OH groups with extraframework Al species or structure defects with Lewis acidity [36]. Lastly, low acid site densities penalize the bimolecular demanding mechanism [37–40], hence increase the relative significance of protolysis.

Protolytic cracking and dehydrogenation of alkanes involving steps in which C–H and O–H bonds are broken and formed, the rate of H/D exchange between light and deuterated reactants can yield information on the nature of the kinetically limiting steps [41,42]. The rate of exchange between $n(\text{H}_{10})$ – $n(\text{D}_{10})$ butane molecules and between (H_8) – (D_8) propane molecules over HMFI at high temperatures (450–550 °C) was found to be 1–2 orders of magnitude higher than the rates of protolytic cracking and dehydrogenation. Hydrogen exchange proceeds stepwise, i.e., only one H (or D) of the substrate is exchanged in a single catalytic turnover. The activation energy of exchange was found lower than those of dehydrogenation and cracking: $\sim 80 \text{ kJ mol}^{-1}$ against 115 and 135 kJ mol^{-1} . Therefore, the C–H bond activation step of alkanes which is involved in alkane dehydrogenation cannot be the kinetically limiting step of this reaction. HMFI activates C–H bonds very effectively but it cannot dispose rapidly of the resulting hydrogen atoms. Therefore, according to Biscardi and Iglesia [43,44] these atoms are used to re-hydrogenate hence to desorb carbenium ions from the zeolite surface.

H/D exchange between light propane or isobutane and deuterated acid catalysts: zeolites, sulfated zirconia, heteropolyacids was also investigated but at lower temperatures ($<300 \text{ °C}$ and

generally $<100 \text{ °C}$). As could be expected, H/D exchange under these conditions was shown to proceed through the carbenium ion-chain mechanism [45,46,47].

The first stages of propane 2- ^{13}C activation were examined by ^{13}C MAS NMR [48]. Scrambling of ^{13}C was shown to occur at short reaction times ($>5 \text{ min}$) at 300 °C . To explain this scrambling two parallel transformations of protonium ions resulting from propane protonation over strong acid sites were proposed: isomerization into C-ethanemethonium ions and transformation into H_2 and isopropyl carbenium ions which rearrange into cyclopropanium ions both followed by propane desorption.

Theoretical chemistry allowed some advances in the description of the transition states of protolysis. Kramer et al. [49] were the first to infer about the features of adsorbed carbonium ions for the methane H/D exchange reaction. According to their results, carbonium ions were highly energetic transition states, stabilized by nearly covalent interactions of two of their protons with two partially negative framework oxygen atoms bonded to aluminum atoms. Kazansky et al. [50,51] and Collins and O'Malley [52–54] reached to similar conclusions for the protolysis of methane, but also of ethane (Fig. 4), propane and butane. Moreover, their calculations also indicated that carbonium ions with more than two carbon atoms would crack to form an alkane and an alkene instead of an alkoxide species. Similar conclusions were drawn by other authors [22,23,55–59].

2.1.3. Conclusion

It is now well admitted that over acid zeolites, the activation of light alkanes may occur not only through the classical carbenium ion-chain mechanism but also through protolysis of the C–H or C–C bonds via carbonium ion transition states. However, some observations such as the apparent limitation of protolytic dehydrogenation by hydrogen desorption are not completely understood. Over constrained zeolites

Table 1
Primary products in the cracking of ethane, propane, *n*-butane and isobutane over H-MFI at 500 °C [31]

Alkane	C_2H_6	C_3H_8	<i>n</i> - C_4H_{10}	<i>iso</i> - C_4H_{10}
Primary products	$\text{C}_2\text{H}_4 + \text{H}_2^{\text{a}}$ CH_4	$\text{C}_3\text{H}_6 + \text{H}_2^{\text{a}}$ $\text{CH}_4 + \text{C}_2\text{H}_4$ (1:1)	$\text{C}_4\text{H}_8 + \text{H}_2^{\text{a}}$ $\text{CH}_4 + \text{C}_3\text{H}_6$ (1:1) $\text{C}_2\text{H}_6 + \text{C}_2\text{H}_4$ (1:1)	$\text{C}_4\text{H}_8 + \text{H}_2^{\text{a}}$ $\text{CH}_4 + \text{C}_3\text{H}_6$ (1:1)

^a Not quantitatively analyzed.

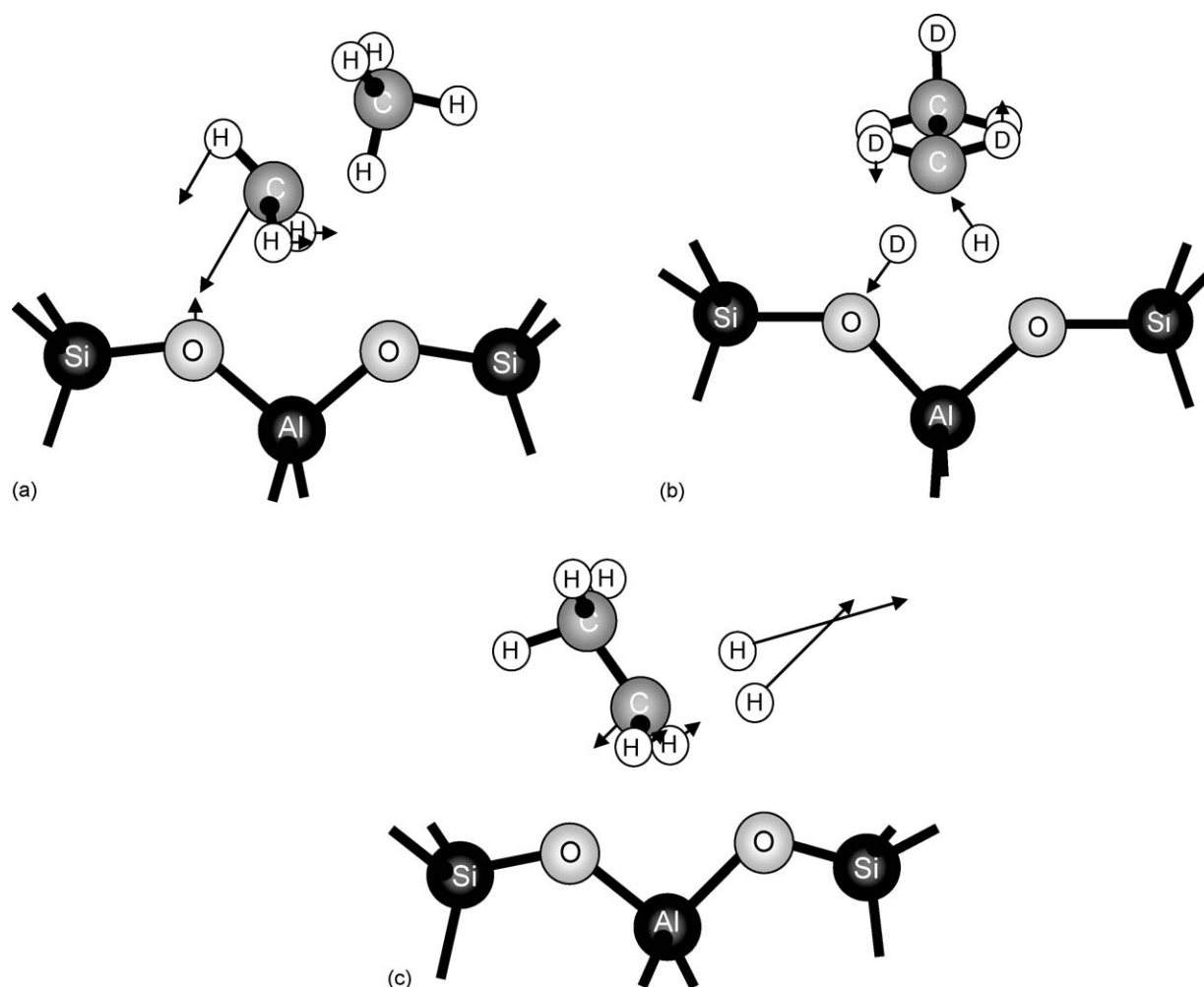


Fig. 4. Transition states and reaction coordinates (main components for the displacement of the atoms along the reaction coordinate) represented by arrows for: (a) protolytic cracking, (b) hydrogen–deuterium transfer and (c) dehydrogenation of ethane. Adapted from [57].

such as HMFI, at high temperatures (>500 °C) and low conversions, essentially the products expected from protolysis can be observed, whereas over non-constrained zeolites (e.g. HFAU), particularly at low temperatures and high conversions, protolysis only participates as initiation step of the carbenium ion-chain mechanism.

2.2. Disproportionation and isomerization

On protonic zeolites, disproportionation of pure C₃–C₄ alkanes appears around 250 °C; ethane remains practically unreactive [60]. Propane is much less reactive than *n*-butane (50-times over HMOR) leading essentially to an equimolar mixture of ethane and butanes. From *n*-butane, isobutane is formed in addition to the disproportionation products: propane and pentanes [60].

2.2.1. Reaction mechanism

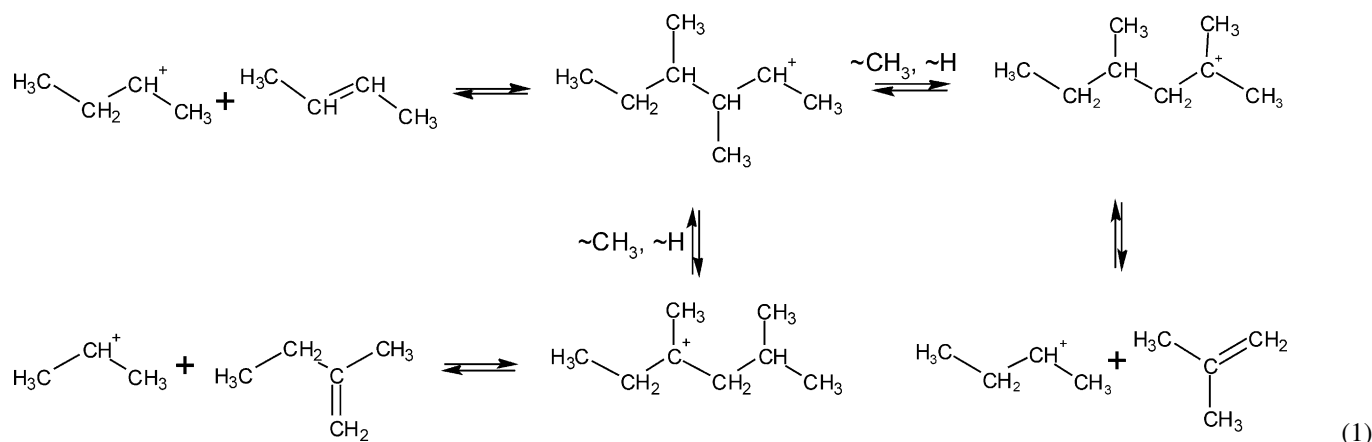
n-Butane transformation was mainly investigated over HMOR zeolites which, owing to their high acid strength are the most active zeolite catalysts for *n*-butane isomerization (a commercially important process). Therefore, low operating tem-

peratures could be used, which because of thermodynamic constraints constitutes a significant advantage [8].

Under the following conditions: fixed bed reactor, 250 °C, butane partial pressure <0.1 bar, nitrogen being used as a diluent, there is an initial increase in activity followed by a slow decrease. After the initial period of activation, an apparent kinetic order with respect to the reactant (*n*-butane or isobutane) close to 2 was found for both isomerization and disproportionation over HMOR 10 (Si/Al = 10). It can therefore be concluded that both reactions occur through the same bimolecular mechanism [60].

The carbenium ion-chain mechanism [7] presented in Fig. 5 shows how *n*-butane can be transformed by similar steps into isobutane or into propane and pentanes. Five different steps are involved: formation of butyl carbenium ions through hydride transfer from *n*-butane molecules to pre-existing carbenium ions R⁺ (step 1), desorption of *n*-butene molecules from the protonic sites (step 2), reaction between butyl carbenium ions and *n*-butene molecules with formation of octyl carbenium ions (step 3), rearrangement of these ions (step 4) then cracking of the rearranged ones (step 5), lastly desorption of alkanes (steps 6 and 6' from the C₃, C₄, C₅ carbenium ions and olefins resulting from step 5). It should be remarked that steps 6 and 6' are identical

to the reverse of step 2 and to step 1, respectively, hence that the carbenium ions R^+ involved in step 1 are those of steps 6 and 6'. All the steps of this bimolecular mechanism involve only secondary and tertiary carbenium ions as transition states, hence are facile to be catalyzed. With this mechanism, the only way to account for the value of 2 of the reaction order is to admit that the limiting step is bimolecular, which is only the case for step 3. Furthermore, the initial period of activation could correspond to a progressive increase of the concentration of the R^+ carbenium ions.



A very important remark is that through this mechanism isobutane and propane plus pentanes should be simultaneously formed as apparent primary products, in contradiction

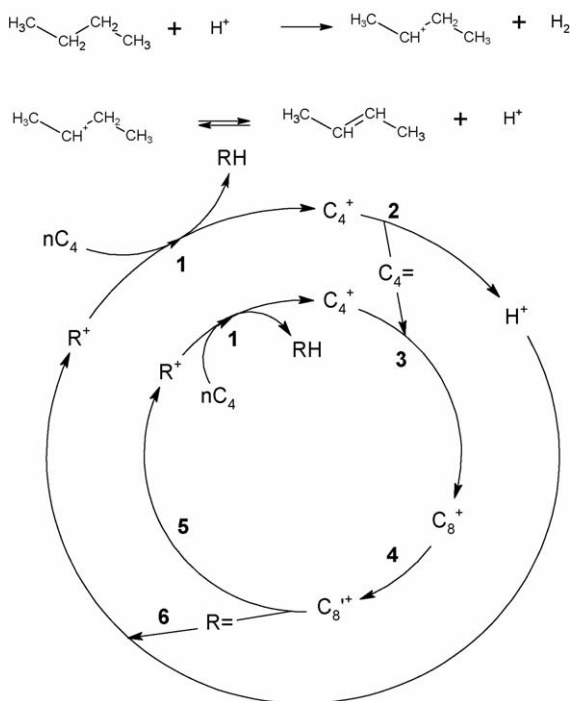
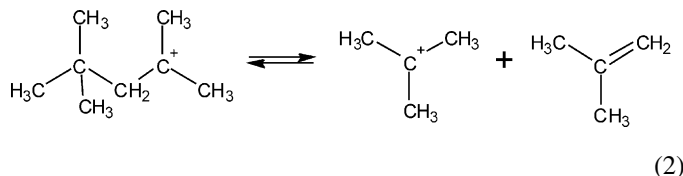


Fig. 5. Mechanism of *n*-butane isomerization over HMOR zeolites: initiation steps and carbenium ion-chain mechanism. $R^=$, R^+ , RH: alkene intermediates, carbenium ion transition states and alkane products (isobutane, propane and pentanes).

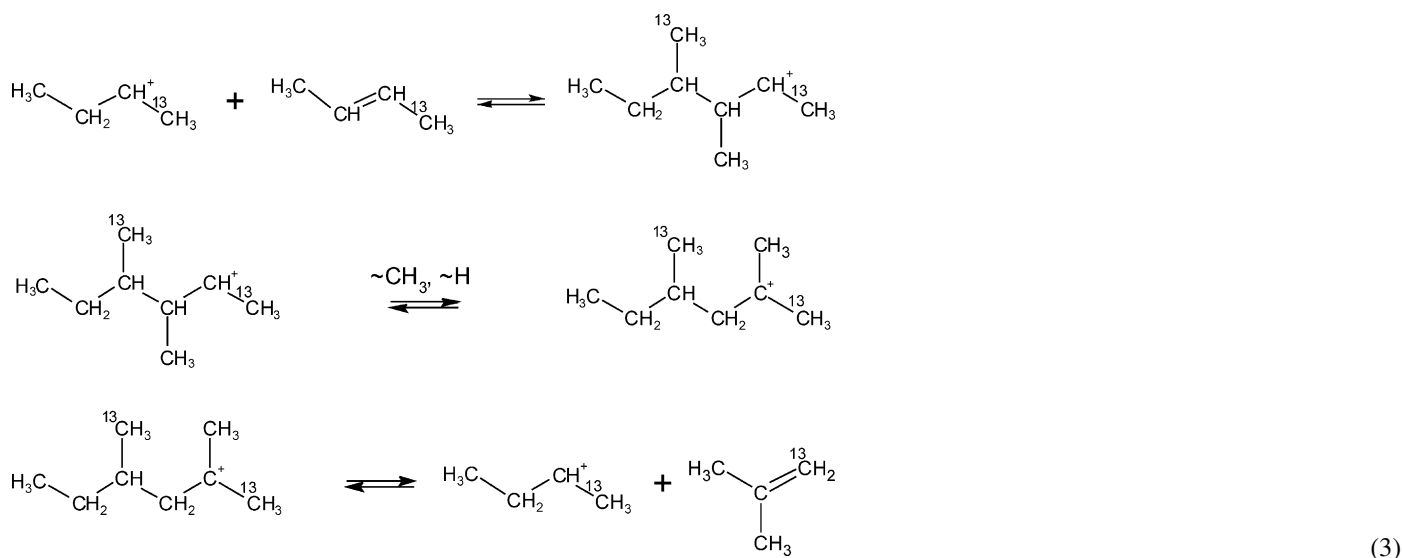
to what was sometimes proposed, i.e., that isobutane is a primary product, whereas propane and pentanes would be secondarily formed. An example is given below (Eq. (1)) showing that both formations of isobutane (*n*-butane) and propane + pentanes can involve the same steps: type-A isomerization (through alkyl shift) and type-B cracking (i.e., with the intervention of one tertiary and one secondary carbenium ions)

Another important point to be underlined is that the selectivity to isobutane should depend on the degree of isomerization of the C_8^+ carbenium ions. If isomerization occurs only through alkyl shift (type A isomerization), the selectivity will be low (only $\sim 33\%$) because the formation of propane + pentanes and isobutane + *n*-butane involves the same steps and the same carbenium ions (Eq. (1)), hence should occur at similar rates. On the opposite, if all the C_8^+ carbenium ions can be formed, which requires type B isomerization (i.e., through protonated cyclopropane transition states), isobutane will be formed through a very facile type A cracking step (i.e., which involves two tertiary carbenium ions) (Eq. (2)),



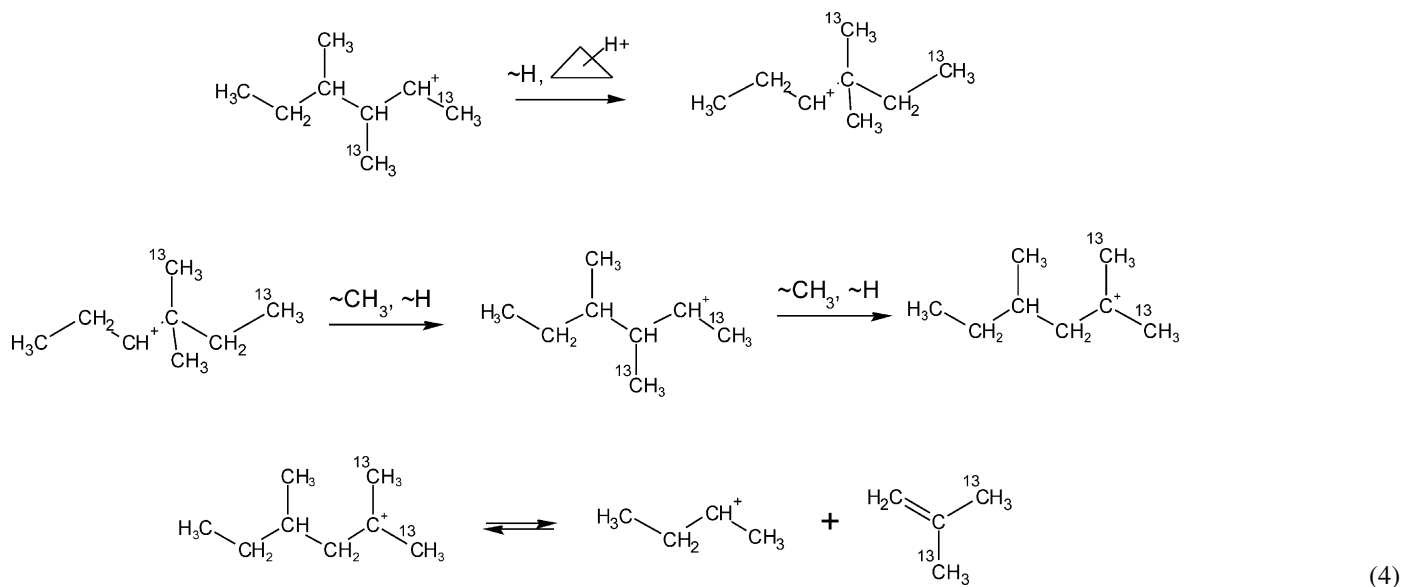
although the formation of propane + pentanes will occur necessarily through the more difficult type B cracking steps.

Experiments with ^{13}C labelled reactants: $[1-^{13}C]$ *n*-butane, $[1-^{13}C]$ and $[2-^{13}C]$ isobutane confirm the bimolecular isomerization mechanism [61]. Indeed the isomerization products contain more species with no or two ^{13}C atoms than the reactant [7], hence cannot result (only) from a monomolecular process. Furthermore, the facile type A rearrangements [15] are not enough to explain the formation of these species (Eq. (3)):

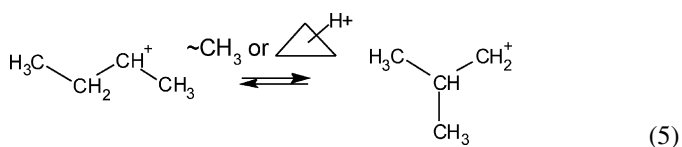


Therefore, the rearrangement of octyl carbenium ions (step 4) of Fig. 5) involves not only type A rearrangements but also several type B rearrangements (Eq. (4)), which could explain the high selectivity to isobutane.

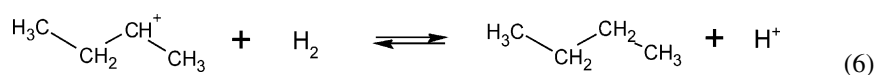
lower, ~15-times more than that of the bimolecular one. This is not surprising, the monomolecular process of *n*-butane isomerization involving very unstable primary carbenium ions as transition states (Eq. (5)):



The effect of hydrogen on *n*-butane transformation [62,63] suggests the possibility of a monomolecular isomerization of *n*-butane over HMOR zeolites. Indeed hydrogen has a significant inhibiting effect on *n*-butane isomerization: apparent reaction order of ≈ 1 . Furthermore, under hydrogen there is no more activation period, the selectivity to isobutane is greater and the order with respect to *n*-butane equal to ~ 1 (instead of 2 under nitrogen) as could be expected from a monomolecular process. However, the rate of this process was estimated to be much



The inhibiting effect of hydrogen on the bimolecular transformations of *n*-butane was explained [62,63] by a large decrease in the concentration of the *sec*-butyl carbenium ions caused by the following reaction (Eq. (6)):



which reduces significantly the rate of the limiting step (step 3) in Fig. 5) of the bimolecular mechanism.

In the mechanism described in Fig. 5, the alkenes corresponding to the reactant are involved as intermediates. This explains why the addition of a small amount of isobutene to isobutane increases significantly the initial rate of isobutane transformation [64–67]. An increase can also be observed when propene or ethene are added to isobutane. This could be expected since these olefins are rapidly transformed into carbenium ions R^+ which can participate through hydride transfer in the formation of *tert*-butyl carbenium ions. Besides this positive effect on the initial rate, the addition of alkenes has a negative effect on the catalyst stability [68].

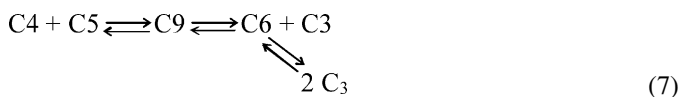
Some authors [66] have proposed that isomerization and disproportionation of isobutane over HMOR zeolites occur only in presence of alkene traces in the feed. However, the formation of a small amount of methane and hydrogen which is generally observed, is a strong argument in favour of alkane protolysis on the strong protonic sites of HMOR zeolites as initiation step (Fig. 5), hence against this proposal [67].

2.2.2. Influence of the acidity and pore structure of the zeolite catalysts

Experiments with pyridine poisoning or exchange by sodium ions of a HMOR(10) sample show that only a small fraction of the protonic sites (the strongest ones) are active in butane transformation [7]. In agreement with that, a USHY zeolite with a Si/Al ratio of 5 whose acid sites are weak in comparison to those of HMOR samples was found to be 110-times less active than HMOR(10) at 350 °C. Moreover, at lower temperatures, no transformation of pure butane could be observed over this USHY zeolite [69,70].

n-Butane transformation under nitrogen was carried out over a series of HMOR samples with Si/Al ratios of ~7 (non-dealuminated sample), 10, 20, 60 and 80 (resulting from dealumination) [71]. A linear relation was found between the activity of these samples (except HMOR7) and the square of the concentration of the protonic sites, which suggests a demanding process, i.e., requiring two acid sites for its catalysis. This seems possible, two acid sites being involved in step 1 of the bimolecular mechanism (Fig. 5). However, these acid sites do not need to be adjacent as originally advanced.

HMOR(7) was not only less active (5 times) than expected from its protonic site concentration but the selectivity to isobutane was much lower (only 25% at low conversions) than over the dealuminated samples (70–80%) essentially at the benefit of propane [71]. The low activity and selectivity of HMOR(7) could be related to the absence of mesopores in this non-dealuminated sample and therefore to the much longer diffusion pathway for hydrocarbon molecules. As a consequence whereas the reactant molecules diffuse along the channels they can undergo many successive bimolecular reactions with a preferential formation of propane. Indeed butanes and pentanes are more reactive than propane and can be transformed into this product (Eq. (7)):



This type of shape selectivity related to the unidirectional pore system of mordenite, which was found for the first time in xylene isomerization over Al-containing MCM41 samples, was called tunnel-shape selectivity [72,73]. This shape selectivity can also account for the low apparent activity of HMOR7. Indeed the transformation in a large channel of each *n*-butane molecule involves all the protonic sites of this channel, which therefore appear to have a low efficiency.

The “diameter” of the channels of mono-dimensional zeolites has a very significant effect on activity and selectivity [74]. Thus, the turnover frequency of the protonic sites decreases significantly from 7–14 h⁻¹ with HMOR ($\varnothing=4.5\text{--}7 \text{ \AA}$) to 0.13 h⁻¹ with HTON ($\varnothing=4.6 \times 5.7 \text{ \AA}$) and 0.06 h⁻¹ with HFER ($\varnothing=4.2 \times 5.4 \text{ \AA}$). At ~250 °C, the selectivity to isobutane of TON is slightly smaller than that of HMOR (~70% against ~80%), whereas that of HFER is very low (~5%), the products expected from a monomolecular cracking and especially ethane and methane being predominant. Diffusion limitations could explain from a large part the apparent low activity of the protonic sites of HTON and HFER. With this latter zeolite, steric constraints could also limit the formation of bimolecular intermediates.

It is probably for the same reasons that the protonic sites of HMF1, a tri-dimensional average pore size zeolite ($\varnothing=5.1 \times 5.5 \text{ \AA} \leftrightarrow 5.3 \times 5.6 \text{ \AA}$), were found to be 15-times less active than those of HMOR and that the selectivity to isobutane was very low (propane was the major product) [74,75].

2.2.3. Conclusion

Owing to the high acid strength of their protonic sites and to the relatively large diameter of their channels, HMOR zeolites are the most active and selective zeolites for *n*-butane isomerization. The presence of mesopores which limit the length of the diffusion path is however indispensable to reach the optimal activity and selectivity. These mesopores which make the pore structure quasi tri-dimensional [76] have also a significant effect on the catalytic stability. With this zeolite at least at low temperatures (~250 °C), *n*-butane transforms essentially through a dimerization–isomerization–cracking mechanism. A very small part of *n*-butane isomerization seems to occur through a monomolecular mechanism. However, the existence of this mechanism deserves to be confirmed and the nature of the corresponding transition state (either carbonium or carbenium ions) to be specified.

2.3. Light alkanes aromatization

The alkenes resulting from protolysis of light alkanes or/and from hydrogen transfer reactions are very reactive in acid catalysis. Therefore, at the high temperatures required for their formation over acid zeolites, they can undergo various secondary reactions leading to thermodynamically stable products, i.e., aromatic hydrocarbons. These hydrocarbons formed in the zeolite micropores can, depending on their properties (size and polarity) and on those of the pore system, either desorb or remain trapped. In this latter case, these compounds (called carbonaceous deposits or coke) limit or block the access to the active

sites with as a consequence a decrease in activity [77]. This decrease in activity can be very fast (e.g. mono-dimensional zeolites or zeolites with trap cages, i.e., large cages with small apertures), slow and even very slow. MFI is an example of zeolite for which the deactivation by coking is very slow owing to its tridimensional pore system and to a size of channel intersections (\approx cages) close to the size of the channel diameters: practically all the molecules formed at these channel intersections can diffuse in the channels [78]. Another advantage of this zeolite, well demonstrated in the methanol to gasoline process (MTG), is the limitation by steric constraints at the channel intersections of the growth of bulky products with as a consequence essentially the formation of valuable benzenic hydrocarbons. It is why most of the studies of alkane aromatization were carried out over MFI zeolites. Nevertheless the medium pore size MEL zeolite which has similar characteristics: tridimensional, no trap cages can also be used [79].

2.3.1. Reaction scheme

The alkane aromatization process can be divided in two stages: the transformation of light alkanes into olefinic products which was described above and the transformation of these olefinic products into aromatic hydrocarbons (see propane aromatization scheme in Fig. 6). The second stage proceeds through a number of reactions involving alkoxide intermediates and carbenium ions as transition states. Ethylene and propene resulting from propane transformation (first stage in Fig. 6) undergo oligomerization–cracking reactions leading to C_4 – C_{10} olefins. Hydrogen transfer from these olefins to other olefins leads to the formation of the corresponding dienes (and of alkanes). Dienes undergo cyclization (intramolecular oligomerization), the resulting cycloalkenes being transformed into cyclic diolefins by

hydrogen transfer. The last step is the transformation of cyclic diolefins into aromatics through hydrogen transfer (a stoichiometric dehydrogenation could also be possible at the high reaction temperature). An important remark is that as a consequence of the hydrogen transfer steps involved in aromatization (steps 2, 4, 6 and 7 in Fig. 6), aromatic formation is balanced by the formation of alkanes at the expense of alkenes, with therefore a limitation in aromatic production.

Kinetic modeling of propene [80] and of propane [81] aromatization over HMF1 allows an estimation of the rate constants of the various steps of Fig. 6. Olefin formation (steps 1 and 2) was found to be kinetically limiting [82,83] in agreement with the much higher reactivity of alkenes compared to alkanes. This step was found to be 10^3 -times slower than step 4 (diene formation) which is the slowest step of propene aromatization. Diene formation is 10^5 -times slower than the fastest step (step 7), aromatic formation) and 10^4 – 10^5 times slower than oligomerization–cracking (step 3), diene cyclization and cyclic diolefin formation (step 6) [80].

As shown above for protolysis, the rate of aromatization depends very much on the alkane reactant. Furthermore the desired aromatic products are accompanied by a large amount of alkanes resulting from both protolysis and hydrogen-transfer reactions. Nonetheless, an aromatization process was developed by Mobil for converting light hydrocarbons to BTX aromatics over a HMF1 catalyst. However, in this process called M2 forming, the feed is constituted by a mixture of alkanes and alkenes (not by only alkanes) [84]. The aromatics yield is limited by the stoichiometric constraint imposed by the hydrogen contents of feed and products: unsaturated hydrocarbons increase both the global conversion and the yield in aromatics.

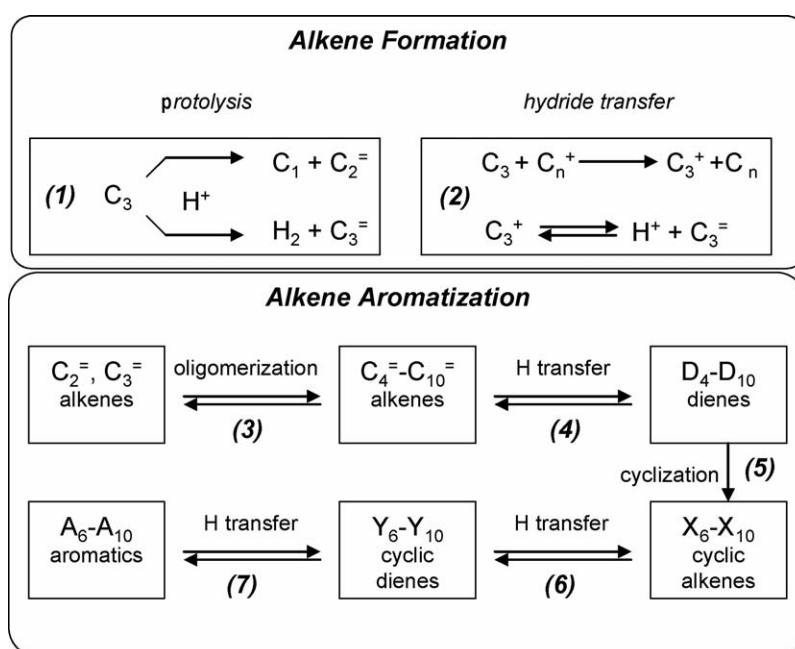


Fig. 6. Pathway of propane aromatization over HMF1 zeolites. Adapted from [81].

2.3.2. Conclusion

At high temperatures (>500 °C), purely acidic zeolites are able to catalyse the aromatization of light alkanes, with however two major drawbacks: (i) their deactivation by carbonaceous deposits which is generally very fast, except however with constrained zeolites such as HMFI and HMEL and (ii) their selectivity to aromatics which is very poor due to alkane formation both by protolytic cracking and by hydrogen transfer from aromatic precursors to olefin intermediates.

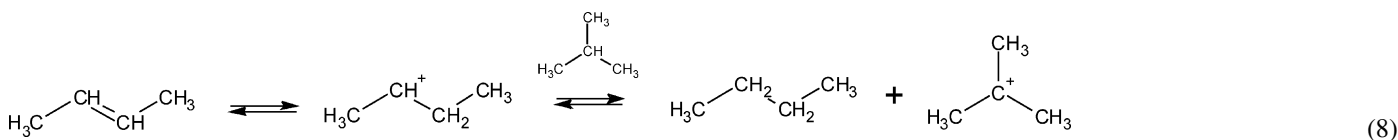
2.4. Alkylation of isobutane with *n*-butene

The alkylate resulting from conversion of isobutane/*n*-butene mixtures is a highly desirable high octane gasoline cut [8,85–89]. The established alkylation technologies use either concentrated sulphuric acid or anhydrous hydrofluoric acid catalysts, with obvious security and environmental concern. There is therefore a genuine desire to develop more environment-friendly catalysts. Much effort has been put in the search for a solid alkylation catalyst with unfortunately relatively little success. Zeolites were the most investigated, the main problem in their use being their fast deactivation. It is why after a short presentation of alkylation chemistry, essentially the recent advances in deactivation and regeneration of zeolite catalysts will be discussed.

2.4.1. Chemistry of alkylation

Alkylation is a very complex process leading as expected (from isobutane and *n*-butene reactants) essentially to trimethylpentanes but also to a large variety of other desorbed products with a number of C atoms between 4 and 14 and to non-desorbed products [8,85–89]. On the fresh zeolite catalysts, butene can be totally converted, with formation of five families of alkanes: *n*-butane and four families with tertiary carbon atoms: C₅–C₇ (called light ends), the desired trimethylpentanes (TMP), other C₈ alkanes, mainly dimethylhexanes (DMH), C₉–C₁₄ alkanes (heavy ends). After a certain reaction time, butene conversion begins to drop with simultaneously a significant change in the product composition with appearance of C₈ alkenes resulting from butene dimerization. A plateau of conversion is finally reached at which essentially these C₈ alkenes can be observed [86]. Only weak protonic sites are needed for this very facile reaction of dimerization (cf Section 2.3.1), whereas alkylation would require strong sites.

The classical alkylation cycle advanced to explain the formation of TMP from an isobutane/*n*-butene mixture is presented in Fig. 7. Three types of steps would be involved: butene addition to *tert*-butyl carbenium ions (step 1), isomerization through H shift (2a) and/or CH₃ shift(s) (2b), hydride transfer from isobutane to the C₈ carbenium ions (step 3). The initiation step of this carbenium ion-chain mechanism is the hydride transfer (HT) from isobutane to *sec*-butyl carbenium ions resulting from butene protonation (Eq. (8)):



HT to secondary carbenium ions such as the *sec*-butyl carbenium ions is known to be much slower than HT to tertiary carbenium ions (e.g. step 3), which explains that except butane, only alkanes with tertiary carbon atoms can be observed in the products.

Although 2,2,3-TMP should be the primary product of alkylation, the selectivity to this product is always quite low (<10% of the TMP). Several explanations could be advanced to explain this observation: namely steric difficulty in the approach of isobutane from the positive charge of the corresponding carbenium ion which is protected by the *tert*-butyl groups [90], participation of other reactions in the formation of TMP. This latter proposal is most likely, for 2,3,3-TMP is primarily formed in large amounts over a USHY zeolite although the corresponding hydride transfer should suffer from similar steric constraints as the one leading to 2,2,3-TMP. The comparison of isobutane/*n*-butene and isobutane/propene transformations over a USHY zeolite demonstrates the existence of a self-alkylation of isobutane with formation of 2,2,4-TMP [91]. The mechanism of this reaction developed in reference [91] involves successively the formation of isobutene from *tert*-butyl carbenium ions, the addition of this olefin on the *tert*-butyl carbenium ion, then hydride transfer. Other reactions are necessary to explain the formation of all the products:

- Dimerization of *n*-butenes followed by hydride transfer to account for the dimethylhexane products.
- Alkylation of C₈ carbenium ions by butene molecules followed by cracking and hydride transfer to account for the heavy and light ends.
- Formation of heavy unsaturated species responsible for the deactivation of the strong acid sites with change from alkylation to oligomerization reactions.

2.4.2. How to limit deactivation?

All the authors agree that deactivation is due to the formation and retention within the zeolite micropores of heavy products. Of course, the knowledge of their composition and of their effect on the active sites (poisoning, blockage of their access) is indispensable for finding ways to increase the catalyst stability and to design an efficient regeneration method [86].

Despite of that, there are few studies devoted to the characterization of carbonaceous deposits and of the deactivated zeolite catalysts. The characterization techniques that were applied are elemental analysis [92], ¹³C NMR spectroscopy [93–95], FT-IR spectroscopy [95–101], UV–vis spectroscopy [92,95,100,101], temperature programmed oxidation [100–103], matrix assisted laser desorption/ionization time-of-flight mass spectroscopy (MALDI-TOF) [99] and dissolution of the zeolite in HF solution with subsequent extraction and analysis of the organic phase [96,99] by GC, FT-IR, H NMR, MS and GC/MS coupling. Note that only the characterization of the carbonaceous deposits after

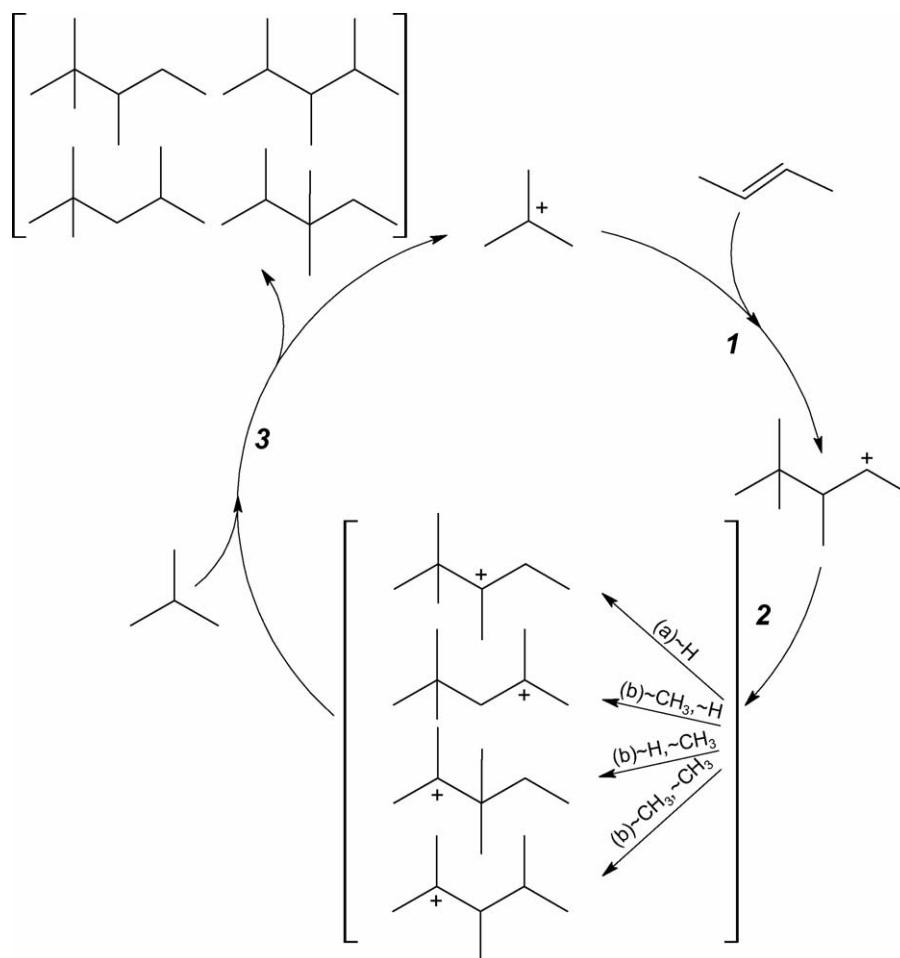


Fig. 7. Production of trimethylpentanes (TMP) by alkylation of isobutane with 2-butene. Catalytic cycle.

separation from the zeolite can lead to their composition, i.e., the distribution of their components as a function of their nature and of their size. However, the characterization of the deactivated catalysts is also indispensable, in particular for specifying the interaction between the molecules of carbonaceous compounds and the acidic sites.

The composition of the carbonaceous deposits depends on the operating conditions, and especially on reaction time and operating temperature [99]. Whereas, there are some differences in the conclusions of the studies, most of the authors agree with the presence of heavy (up to 30 [96] or to 35 [99] C atoms), unsaturated highly branched species containing cycles. The atomic H/C ratio measured by Klingmann et al. [92] was equal to 1.6, whereas a slightly higher value 1.7–1.8 can be deduced from the results of other studies [96,99]. According to Feller et al. [99], aromatic compounds are present in carbonaceous compounds, their amount increasing with reaction temperature, whereas no aromatics were found by others [92,96]. The number of unsaturations in the carbonaceous compounds was concluded to be 2 from the presence of a band at 305 nm in the UV–vis spectrum originating from monoenylic carbocations [92]; on the other hand, from hydrogenation of carbonaceous compounds, Pater et al. [96] suggested the presence of only one double bond.

IR spectroscopy analysis of the “coked” zeolite samples shows that coke molecules interact with the protonic sites: indeed there is a partial or a complete disappearance of the bands corresponding to the bridging hydroxyl groups [96,99]. This interaction is responsible for the catalyst deactivation through poisoning of the acidic sites at high temperatures (130 °C) and probably through pore blocking at low temperatures (40 °C) [99].

Condensation reactions are necessarily involved in the formation of the carbonaceous deposits. Therefore, limiting the growth of product molecules seems one of the best ways to increase the catalyst lifetime. Bulky molecules can result from oligomerization or from alkylation of octyl carbenium ions (C_8^+) precursors of TMP by butene molecules. Trimerization of butenes or monoalkylation of C_8^+ lead to C_{12} carbenium ions which are precursors of light and heavy ends. However, these C_{12} carbenium ions can also lead by alkylation with butene to heavier compounds. All these reactions of condensation are similar to oligomerization. It is why most of the authors agree with the proposal that the lifetime of the alkylation catalyst is mainly determined by the relative rates of hydride transfer (HT) and of oligomerization (O) [104]. The higher the HT/O ratio the greater the yield in alkylation products and the smaller the formation of carbonaceous deposits hence the slower the deactivation. It

should be noted that this condition is not easy to be satisfied for the rate constant of oligomerization is much greater than the rate constant of hydride transfer: 2 [104] to 3 [105] orders of magnitude.

However, a stability increase can be obtained by an adequate choice of the zeolite catalyst, of the reactor and of the operating conditions [86,90,104]. Thus, hydride transfer requires strong acid sites with in addition a significant positive effect of their density [37–40]; moreover, this reaction involves a bulky bimolecular transition state. As a consequence, a large pore zeolite such as FAU with the greatest possible concentration of acidic sites (e.g. *X* rather than *Y*) will be chosen. TMP molecules being relatively bulky limitations in their desorption from the zeolite micropores [106] could occur with therefore an increase in the secondary reactions of condensation involved in the formation of carbonaceous deposits. The use of zeolites with small crystallites will reduce these limitations. Thus, the small size of the HBEA crystals could be one of the reasons for the good stability of this zeolite [106]. Lastly the significance of oligomerization which involves two or more molecules of butene will be lower if *n*-butene concentration is kept very low throughout the reactor. This could be achieved by using a continuous stirred tank reactor (a fixed bed reactor is not suitable) with high isobutane/*n*-butene ratios and low *n*-butene space velocities [86,90,104]. Reaction temperature was also shown to have a significant effect on the lifetime with a maximum at 75 °C (over a LaX catalyst). Faster deactivation at low temperatures would be due to diffusion limitations with catalyst deactivation by pore blocking, whereas at high temperatures it could be due to a faster formation of highly unsaturated compounds which strongly adsorb on the active sites (site poisoning) [90].

2.4.3. Novel regeneration methods

Due to the rapid deactivation of zeolite catalysts, and that despite the recent advances (Section 2.4.2), all the industrial alkylation processes using these catalysts will require a periodical (or even a continuous) regeneration. Oxidative treatment is classically used to remove carbonaceous deposits from zeolite catalysts. However, this technology which is well adapted to the removal of coke from the hydrothermally stable zeolite catalysts employed in high-temperature processes presents as major inconveniency when applied to the low Si/Al alkylation zeolite catalysts to decrease their acid site concentration, and consequently their activity and lifetime. Indeed whereas owing to their high hydrogen content ($H/C = 1.6\text{--}1.8$), these deposits could be expected to be oxidized at low temperatures, they undergo upon heating a change in their structure. Their unsaturated aliphatic components adsorbed on the protonic sites are easily transformed into aromatic compounds which require high temperatures for their oxidation. It is why novel methods were investigated to remove the carbonaceous deposits from the alkylation zeolite catalysts: oxidation with ozone or with hydrogen peroxide [104], hydrocracking [92,103,107], supercritical fluid extraction [100,101,108–113], promising results being obtained with the last two methods.

Regeneration by hydrocracking, patented 30 years ago [114] was investigated by two groups [92,103,107,115] and more par-

ticularly by the group of Weitkamp. The operating conditions for a complete restoration of the activity were determined from an in situ FT-IR study, the alkylation catalyst (LaX) being doped with 0.4 wt.% Pt [107]. Hydrocracking at a hydrogen pressure of 15 bar and temperatures up to 300 °C was found to restore completely the activity and the selectivity: both the duration of complete conversion of 1-butene and the product composition were identical in four cycles of alkylation–regeneration [107]. However, this regeneration technology has as major inconveniencies to require the addition of Pt to the catalyst and hydrogen supply infrastructure, which increases operation and capital costs.

Supercritical fluids have been explored for limiting the deactivation of solid alkylation catalysts by continuously extracting the carbonaceous deposits [116–120]. However, the critical analysis of the papers [120] shows that the increase in catalyst stability which is observed is generally accompanied by a reduction in product quality. More promising was to exploit the extractive properties of supercritical fluids for dissolving and removing carbonaceous deposits, hence for reactivating the zeolite catalysts.

Among a variety of supercritical fluids tested, branched alkanes (isopentane, isobutane) were the most effective owing to their ability (because of their tertiary carbon atoms) to desorb by hydride transfer the heavy unsaturated compounds adsorbed as enylic carbocations. However, the hydride transfer is not possible with too deactivated samples [112] either because of the too small number of residual strong acid sites or to their limited access. In contrast, very promising results were obtained with partially deactivated samples. Thus, a simple batch of USHY zeolite was utilized for up to 23 reactions/regeneration cycle while maintaining 100% of the initial activity [110].

2.4.4. Conclusion

Significant advances have recently been made both in the lifetime of the zeolite catalysts and in their regeneration. Thus, the lifetime was shown to be significantly increased by an adequate choice of the reactor, catalyst and operating conditions. Moreover, a complete restoration of the initial activity and selectivity can be obtained by removal of the carbonaceous deposits responsible for deactivation either by hydrocracking or by supercritical fluid extraction. These advances and the environment-friendly characteristics of zeolite catalysts should lead in the future to the development of new alkylation technologies employing these catalysts.

3. Transformation of light alkanes over metal zeolite catalysts

The introduction of dehydrogenating species into HMFI: Pt, Zn, Ga, etc. increases the rate and selectivity of aromatization. Various commercial processes using bifunctional Ga/HMFI catalysts: cyclar from UOP and BP [121,122], aroforming from IFP and Salutec [123,124], Z-forming from Mitsubishi and Chiyoda [125] have been developed for liquefied petroleum gas (LPG) transformation into BTX hydrocarbons (benzene, toluene, xylenes) with simultaneous formation of a large amount

of hydrogen which is also a valuable product. This has incited many academic teams to investigate the aromatization of light alkanes especially propane over Ga/HMFI catalysts.

Another reason is the complexity of both the reaction scheme and catalyst system. Thus, not only the aromatization scheme is bifunctional in the meaning of Weisz [126], i.e., scheme constituted of successive reaction steps catalyzed independently by dehydrogenating and acidic sites with therefore steps of diffusion of desorbed intermediates from one type of site to another but in addition, the dehydrogenating steps would involve bifunctional sites associating Ga species and protonic acidic sites. Moreover, as is often the case in bifunctional catalysis processes, monofunctional catalytic reactions (over Ga species or over protonic sites) and even stoichiometric reactions can also play a role in the steps of light alkane transformation. Lastly, major modifications of the physicochemical properties of the catalyst can occur during the pre-treatment and even during the reaction, which makes difficult the identification of the actual active Ga sites.

Section 3.1 is essentially devoted to the main aspects of light alkane aromatization over GaHMFI catalysts. However, the effect of other doping metal cations and especially of Zn cations will also be briefly examined.

The first step of light alkane aromatization over GaHMFI catalysts is the alkane dehydrogenation. Thus, it could be envisaged to limit the alkane transformation to the formation of the corresponding alkene. Unfortunately, alkane dehydrogenation is the limiting step of alkane aromatization and the selectivity to alkene is always poor even at low conversion over Ga-containing, proton-poor MFI [127]. Much better results can be obtained over more classical dehydrogenation catalysts based on supported Pt. However, dehydrogenation reactions being highly endothermic ($\Delta H \approx 100 \text{ kJ mol}^{-1}$) are thermodynamically favored only at very high temperatures with as a consequence significant problems of deactivation. An elegant way to bypass the thermodynamic limitations of dehydrogenation is to eliminate selectively the resulting hydrogen from its formation, for instance by oxidation. Furthermore, the discovery of the remarkable catalytic properties of Fe zeolites for the selective oxidation by N_2O of benzene into phenol [128] has led several teams to explore this oxidation route to transform light alkanes (and especially propane) into the corresponding olefins. This review paper being limited to non-oxidative processes, we do not present and discuss the promising results obtained in oxydehydrogenation of light alkanes.

In Section 3.2, the association of a hydrogenating function to the purely acidic zeolites (especially H-mordenite) which are active in *n*-butane isomerization [129] will be shown to lead to significant improvements. The possibility of a direct formation of isobutene from *n*-butane (dehydroisomerization) will also be examined.

Bifunctional catalysis can also be used for the alkylation of benzenic hydrocarbons with small alkanes. This one pot synthesis of valuable alkylaromatic hydrocarbons, presented in Section 3.3, could constitute an economical and environment-friendly alternative to their classical production by alkylation with alkenes.

3.1. Main features of light alkane aromatization

The main part of this paragraph deals with propane aromatization over Ga/HMFI catalysts. However, the differences between the modes of action of Zn and Ga/MFI catalysts will be presented and discussed.

3.1.1. Demonstration (and nature) of a bifunctional aromatization scheme

Bifunctional pathways can be classified in two main categories, either with independent monofunctional sites, hence with desorbed intermediates, or with bifunctional sites, hence without desorbed intermediates. The first one, which involves successive chemical steps on the two types of sites, often redox and acid ones, and diffusion steps of desorbed intermediates from the redox to the acid sites and vice-versa plays an important role in numerous processes of refining, petrochemicals and fine chemicals. The participation of this pathway can be demonstrated by using intimate physical mixtures of the monofunctional components with different concentrations [126,130]. Indeed, despite the separation of the two functions, a synergy effect can be observed, i.e., the activity of the mixtures is definitely greater than the sum of the activities of their components. It is actually the case for propane conversion and aromatization over mixtures of Ga_2O_3 and HMFI pretreated under nitrogen at 600°C [131]. However, this observation is not a definite proof. Indeed, it could also be explained by modifications of one component in presence of the other one during the catalyst activation or during the reaction with an increase of activity. It will be shown later that this type of complication can exist with Ga_2O_3 /HMFI catalysts pretreated under hydrogen or used for a long time in aromatization at high temperatures. It is less likely in the experiments reported in reference [131] for the activities were measured at very short time-on-stream on samples pretreated under nitrogen.

However, to demonstrate without any ambiguity the existence of this type of bifunctional mechanism on the actual aromatization catalysts, the acid and dehydrogenating activities of the physical mixtures of Ga_2O_3 and HMFI have to be estimated after the activation treatment under conditions representative of aromatization, i.e., in presence of hydrogen at high temperatures. If propane aromatization involves successive reactions on independent sites, a curve similar to that represented in Fig. 8a should be obtained [131]. In this figure, the ratio *R* between the activity for propane aromatization and the acid activity is taken as the ordinate and the dehydrogenation/acid activity ratio (De/Ac) as the abscissa. For low values of De/Ac, dehydrogenation is the limiting step, hence the bifunctional activity per acid site is proportional to De/Ac. For high values of De/Ac, the acid reaction is limiting and the bifunctional activity will be proportional to the acid activity, hence *R* will be constant. Whatever the model reactions accounted for estimating the acid and the dehydrogenating activities, *R* was found to increase proportionally to De/Ac. Examples of this linear relationship are shown in Fig. 8b for Ga_2O_3 /HMFI physical mixtures pretreated under nitrogen. The increase of *R* with De/Ac demonstrates the existence of a bifunctional pathway with desorbed intermediates, whereas the

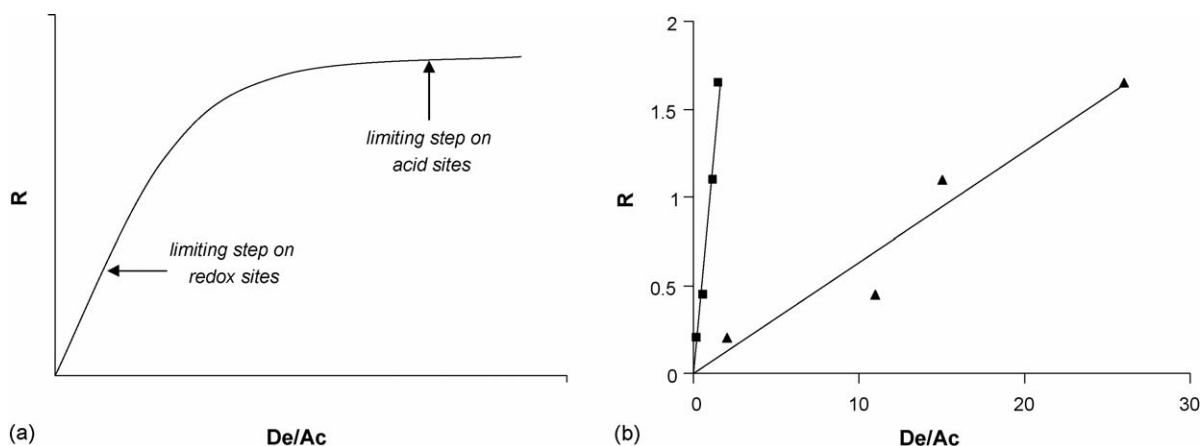


Fig. 8. (a) Expected change of R the ratio between bifunctional/acid activities of classical bifunctional catalysts as a function of De/Ac , the ratio between their dehydrogenating and acid activities. (b) Aromatization/acid activity ratio (R) of mechanical mixtures of Ga_2O_3 and HMFI after pre-treatment under nitrogen at $600^\circ C$ vs. De/Ac . The two straight lines correspond to values of De measured for propane and methylcyclohexane dehydrogenation [7].

linear relationship shows that propane aromatization is kinetically limited by the dehydrogenation steps [131].

The main chemical and physical steps involved in the bifunctional scheme are shown in Fig. 9. Steps 1, 5, 9 and 10 can occur through dehydrogenation, whereas steps 3 and 7 (oligomerization–cracking and cyclization) are necessarily catalyzed by protonic acid sites. Steps 2, 4, 6 and 8 correspond to the migration of desorbed intermediates from dehydrogenation sites to protonic sites and vice-versa. The participation of Ga species in steps 1, 5, 9 and 10 was demonstrated through kinetic modeling of propane and propene aromatization over Ga/HMFI [80,81] catalysts as well as by the use of model reactions [131]. The much higher reactivity of propene compared to propane as well as the apparent direct formation of aromatics from propene are strong arguments in favor of the kinetic limitation of propane aromatization by propane dehydrogenation (step 1 in Fig. 9).

3.1.2. Other reactions involved in propane transformation over Ga/HMFI catalysts

As it is often the case on bifunctional catalysts, the bifunctional pathway is accompanied by monofunctional reactions, here catalyzed either by the protonic sites or by the dehydrogenating species. Thus, as it was demonstrated in propane and propene aromatization over HMFI (without Ga), the zeolite protonic sites are able to catalyze steps 1, 5, 9 and 10 of Fig. 9. Steps 5, 9 and 10 occur essentially through hydrogen transfer from long chain, and cyclic olefins and dienes to light alkenes,

as it was already referred in Section 2.2. On the other hand, step 1 occurs partly through protolysis partly through hydride transfer (Fig. 6). In addition to propene, the protolytic attack of propane yields also methane plus ethylene. Moreover, the competition for adsorption over the protonic acid sites of the aromatic molecules with the less basic paraffinic and olefinic molecules affects significantly the rates of reactions 1, 5, 9 and 10 [80,81].

Furthermore Ga species were shown to be able to catalyze not only the dehydrogenating steps but also propane cracking into methane and ethylene, the hydrogenation of olefins, in particular of ethylene, and the hydrogenolysis of methyl aromatics [80,81,83,132]. A recent study of propane transformation at $500^\circ C$ over different polymorphs of Ga_2O_3 confirms the catalytic activity of this oxide for propane dehydrogenation and cracking [133]. β - Ga_2O_3 which has the largest amount of acidic sites was the most active and selective for propene formation. Gallium oxide being hardly reduced below $600^\circ C$ and the reduced oxide being not restored after O_2 treatment, propane dehydrogenation was proposed to occur (like on ZnO) through a heterolytic dissociation pathway rather than through a redox mechanism. In agreement with this proposal, dihydrogen molecules were demonstrated to be dissociated over Ga_2O_3 into H^+ and H^- species [134]. The results obtained by H_2 (or D_2) adsorption followed by IR spectroscopy are very similar to those found over ZnO [135]. H_2 adsorption gives rise to two IR bands at 3640 and 2020 cm^{-1} , these bands being shifted to 2680 and 1450 cm^{-1} when H_2 is substituted by D_2 . The first one was pro-

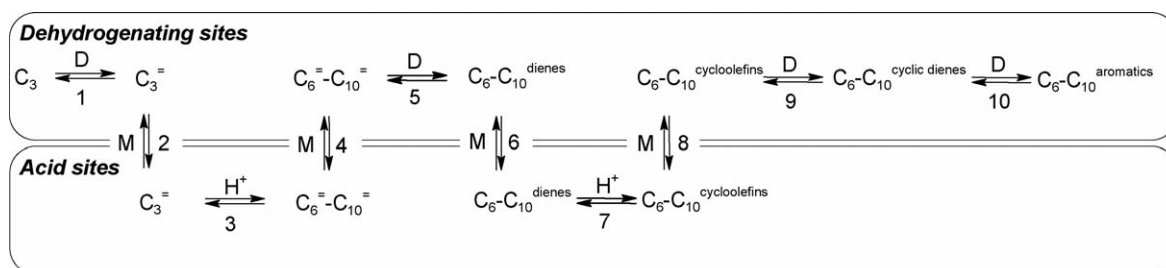


Fig. 9. Propane aromatization over Ga/HMFI catalysts. Bifunctional reaction scheme. (H^+)-protonic sites, (D)-dehydrogenation sites and (M)-migration (diffusion) steps. The dehydrogenating sites are likely bifunctional associating Ga species and protonic sites.

Table 2
Dehydrogenating activity of physical mixtures of Ga₂O₃ and HMFI pretreated at 600 °C under nitrogen or under hydrogen flow

Ga ₂ O ₃ (wt.%)	0	2.7	6.7	13.4	53.8	94.1	100
<i>D_A</i> = “acid activity” (10 ⁻³ mol h ⁻¹ g ⁻¹ zeolite)							
N ₂	5 (1 ^a)	220 (49)	390 (87)	750 (167)	140 (31)	400 (89)	
H ₂	3.2 (1 ^a)	350 (109)	670 (209)	610 (191)	330 (103)	240 (75)	
<i>D_{Ga}</i> = “Ga ₂ O ₃ activity” (10 ⁻³ mol h ⁻¹ g ⁻¹ Ga ₂ O ₃)							
N ₂		7800 (709)	5400 (491)	4800 (436)	130 (12)	25 (2)	11 (1 ^a)
H ₂		12500 (2500)	9300 (1860)	3900 (780)	290 (58)	15 (3)	5 (1 ^a)

The first lines correspond to hypothesis a (“acid activity”), i.e., activation of propane over the zeolite protonic sites with recombinative desorption of H atoms. Lines 3 and 4 correspond to hypothesis b (Ga₂O₃ activity), i.e., activation of propane over the Ga species, the protonic sites facilitating either the desorption of propene, the recombinative desorption of hydrogen or both.

^a Taken as reference.

posed to be due to hydroxyl groups, the second one to gallium hydride species (Ga^{x+}-H).

3.1.3. Dehydrogenation steps. A bifunctional mechanism?

The highest dehydrogenating activity of the β-Ga₂O₃ polymorph was attributed to a conjugated effect of protonic and oxide sites [133]. This synergy effect is well demonstrated in the case of Ga/HMFI catalysts. Thus, Ga₂O₃/HMFI samples are more active in propane aromatization than pure HMFI although Ga₂O₃ is completely inactive [131]. This is mainly due to a synergy effect on propene formation (which, as referred earlier, is the limiting step of aromatization) as furthermore shown in experiments carried out at low propane conversion [131].

Thus, Table 2 shows that for physical Ga₂O₃-HMFI mixtures pretreated at 600 °C either under nitrogen or under hydrogen flow, the value of the dehydrogenating activity per gram of the gallium oxide component (*D_{Ga}*) is much higher for the mixture than for the pure oxide. The smaller the percentage of gallium oxide, the greater the *D_{Ga}* increase, this increase being more pronounced after pretreatment under hydrogen. Thus, for the catalyst with the lowest percentage of gallium oxide (2.7 wt.%), *D_{Ga}* is about 2500- and 700-times greater than for pure gallium oxide after pretreatment under hydrogen and nitrogen, respectively. The continuous increase of *D_{Ga}* with the percentage of the zeolite component in the catalyst could be expected. Indeed the gallium species active in dehydrogenation become more and more close to the acid sites.

Likewise, if the dehydrogenation activity is considered to be due to the acidic sites, the dehydrogenating activity has to be estimated per gram of zeolite (*D_A*). *D_A* was found to be greater with the Ga₂O₃-HMFI mixtures than with the pure zeolite. Here the significance of the synergy effect depends only slightly on the catalyst composition. Nonetheless, an apparent maximum of *D_A* is found for a wt.% of Ga₂O₃ of 13.4 (*D_A* is 170-times greater than for the pure zeolite) and of 6.7 (210-times greater) for the samples pretreated under nitrogen and under hydrogen, respectively. This maximum in the *D_A* value is unexpected, the closest proximity of the acid sites to the gallium oxide which should be favorable to the zeolite activity being for mixtures rich in Ga₂O₃ [131].

Two types of mechanisms were advanced to explain these changes of *D_{Ga}* and *D_A* with the catalyst composition. In the first one (a), propane would be activated over the Ga species

[4,136,137], in the second (b) over the protonic sites [138–142]. However, a third possible explanation could be found in the significant modifications of the catalyst which were found to occur during hydrogen pretreatment or during the reaction (because of hydrogen production) [131,136,143–149]. However, this latter explanation which probably accounts for the increase in the dehydrogenation activity with hydrogen pretreatment (Table 2), does not seem to be valid to account for the change in the dehydrogenation activity of the nitrogen pretreated samples with the catalyst composition. Indeed the activity was measured on fresh catalysts, whereas the catalyst modifications require long-term exposure to the propane reactant [131]. A stronger argument in favor of the bifunctional dehydrogenation mechanism hence against the latter proposal is that the simple exchange by Na cations of a Ga/HMFI sample caused a decrease by more than 2 orders of magnitude (1/180) of the rate of propane dehydrogenation [136].

Fig. 10 shows the mechanism of dehydrogenation proposed by Mériaudeau and Naccache [136]. The first step is the heterolytic dissociation of propane with formation of Ga hydride and Ga alkoxide species. Over pure gallium oxide these alkoxides would decompose into propene and H⁺ bonded to the surface oxygen (step 2); the last step would be the formation of hydrogen from the H⁺, H⁻ species with recovering of the Ga sites. Step 2 would be the limiting step of this catalytic cycle. In presence of the protonic sites at the proximity of the Ga active sites, the propyl carbenium ions formed in step 1 will easily exchange with a zeolite proton through an alkyl surface migration (step 4). This new pathway allows one to bypass the limiting step of propene formation over pure Ga oxide. A slightly different mechanism was proposed by Buckles and Hutchings [150]: propane would be activated at the interface between Ga oxide and protonic sites; the initial process would be the polarization of the C–H bond by Ga oxide, the second one the cleavage of the polarized C–H bond by interaction with the protonic sites. Furthermore, from propane 2-¹³C transformation followed by ¹³C MAS NMR spectroscopy, Derouane et al. [151] conclude to the participation as first intermediate of a protonated pseudocyclopropane species formed by propane activation on a (Ga³⁺, O²⁻) ion pair and its protonation by a nearby protonic acid site. Lastly, according to Ono [4], the role of the protonic sites would be to scavenge the Zn (or Ga) hydride species formed by heterolytic dissociation of propane, e.g. [ZnH]⁺ + H⁺ → Zn²⁺ + H₂.

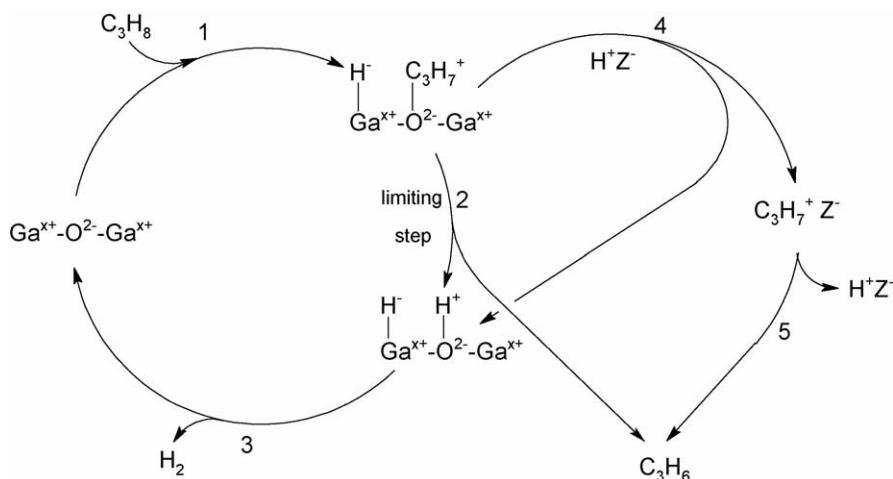
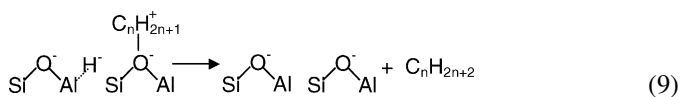
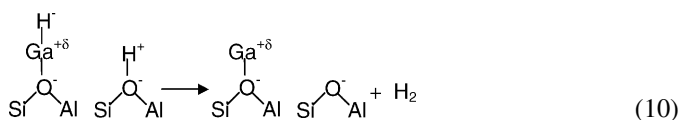


Fig. 10. Ga-acid bifunctional mechanism of propane dehydrogenation over GaHMFI catalysts adapted from reference [135].

In the mechanism proposed by Biscardi and Iglesia [43], the first step is the activation of the C–H bond over the protonic sites, the role of the Ga species being to act as efficient “portholes” for the removal of the H atoms produced during the activation step. To demonstrate this mechanism, reactions of C_3H_8/C_3D_8 mixtures were carried out over HMFI and Ga/HMFI catalysts [43]. Both the roles of propane transformation and of C–H bond activation (cross exchange of D atoms between deuterated and light propane molecules) can be determined from these experiments. Over HMFI, the activation of the C–H bond was found to be much faster (35 times) than propane conversion. This suggests that the protonic sites can activate C–H bonds very effectively but cannot dispose rapidly of the H atoms formed in the C–H bond scission. Therefore, these H atoms are used to hydrogenate surface carbenium ions. Over Ga/HMFI, propane transformation is 3-times faster than over HMFI, whereas the C–H bond activation occurs at similar rates over both catalysts. To explain that, it was proposed that H atoms removal could be achieved not only through H transfer to carbenium ions but also by a re-combinative desorption involving Ga species. Over pure HMFI hydride ions would be momentarily stabilized by adsorption on Al atom sites, these unstable hydride species reacting with carbenium ions to form alkane species (Eq. (9) [140]):



Over Ga/HMFI, the hydride species stabilized by Ga ions would combine with zeolite protons to form H_2 (Eq. (10) [140]):



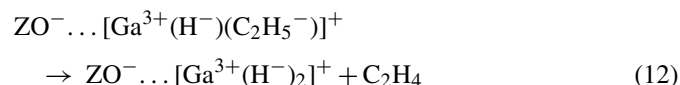
There are no definite arguments in favor of the a or of the b mechanisms. It is furthermore likely that both mechanisms could play a role in dehydrogenation steps over Ga/HMFI catalysts. Whatever it will be, the bifunctional character of the sites

of Ga/HMFI catalysts which are active in dehydrogenation is generally admitted.

However, Ga/MFI samples with Ga under the form of Ga^+ in exchange cations and which contains practically no protons were shown to be active in alkane dehydrogenation. A mechanism was proposed for this dehydrogenation on the basis of the results of diffuse reflectance infra red spectroscopy (DRIFT) experiments with ethane [152]. After heating of Ga/MFI in ethane atmosphere at 250 °C, 4-weak stretching bands appear at 2882, 2914, 2939 and 2962 cm^{-1} which were ascribed to ethyl species grafted to Ga^+ . Another band appears at 2057 cm^{-1} with a shoulder at 2040 cm^{-1} which corresponds to gallium hydride species. The formation of these bands could be described by the following reaction (Eq. (11)):



Prolonged heating resulted in the decomposition of the ethyl species with appearance of new C–H stretchings bands at 3024, 3055 and 3072 cm^{-1} typical of olefin or aromatic hydrocarbons and with a shift of the maximum of the Ga hydride band to 2040 cm^{-1} which indicates the formation of gallium dihydride species as Eq. (12) shows [152].



It should be remarked that in Eq. (11), there is an “alkyl” activation of ethane ($C_2H_5^-$) and not a “carbenium” activation ($C_2H_5^+$) as proposed in the mechanism advanced by Mériaudeau and Naccache [136]. Quantum chemical calculations were undertaken to discriminate between these two possibilities and also to specify the nature of the active Ga species: dihydride gallium ion (GaH_2^+) Z^- or gallyl ion ($Ga=O$) Z^- [153]. The conclusions were that (GaH_2^+) Z^- was the likely active species and that alkane activation occurred via an “alkyl” mechanism involving three successive steps: scission of a C–H bond (1), formation of dihydrogen from the proton and the hydrogen bound to Ga (2) and formation of ethane from the ethyl group bound to Ga [153]. Ethane dehydrogenation over

dihydride gallium ions was recently reconsidered [154], the conclusion being that a one step concerted mechanism was more likely than the three step mechanism proposed by Frash and van Santen [153].

These conclusions on the mode of ethane activation and on the active sites were recently disputed by Joshi and Thomson [155] from a density functional theory (DFT) pathway analysis. Two types of sites were considered: the mono Al site of the form $Z^-[\text{GaH}_2]^{2+}$ (dihydride gallium ion) and a di-Al site: $Z^{2-}[\text{GaH}_2]^{2+}$. With the first type of sites the calculated activation energies were too high compared to experimental values, which leads the authors to conclude that the sites were not likely responsible for alkane dehydrogenation. $[\text{GaH}]^{2+}$ species residing near di-Al sites were proposed to be the active sites. They can be reduced by hydrogen with formation of protonic acid sites (Eq. (13)):



This reaction being endothermic, $[\text{GaH}]^{2+}$ species are predominant at low temperature. However, both species could be present under normal reaction conditions. A carbenium activation mechanism consisting of three distinct steps: activation of the C–H bond with formation of an alkoxide like intermediate (1), desorption of ethene (2) and then of molecular hydrogen was proposed. There is an optimal Al–Al distance due to opposite effects on the activation barrier for C–H activation and for H_2 removal [155]. However, an argument against this proposal of a di-Al route is the low probability of finding Al pairs in the high Si/Al MFI zeolites which are generally used in aromatization.

3.1.4. Composition of the working catalyst

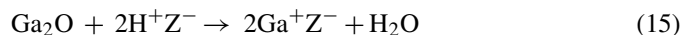
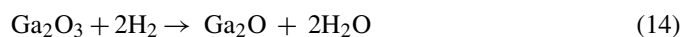
The bifunctional character of the alkane transformation process on Ga/HMFI catalysts and of the dehydrogenating acid sites was shown in Sections 3.1.1 and 3.1.3, respectively. The proposals of the literature on the composition of the Ga/HMFI catalysts under the operating conditions are presented here, the focus being made on the nature of the Ga species.

Gallium can be introduced into Ga/HMFI catalysts through different ways: impregnation with various salts, ion exchange, chemical vapor desorption, mechanical mixtures of Ga_2O_3 and HMFI, synthesis of MFI gallosilicates, etc. Whatever the mode of introduction, Ga can have a beneficial effect on the rate and selectivity of alkane aromatization. All these modes of introduction yield practically always the same type of Ga species after calcination. Thus, impregnation and ion exchange of HMFI lead to the preferential deposition of mostly $\text{GaO}(\text{OH})$ species on the outer surface of zeolite crystallites [156] for hydrated Ga^{3+} cations are too bulky to enter the channels of HMFI [157]; during calcination, these extracrystalline Ga species convert to Ga_2O_3 crystals [142,144,156,158]. Furthermore the calcination of the gallosilicates at high temperatures ($>700^\circ\text{C}$) causes the dealumination of the framework and the formation of extraframework Ga species which deposit on the outer surface of the crystals or within the mesopores under the form of Ga_2O_3 [5,159,160]. The extraframework species were shown to be at least 150-

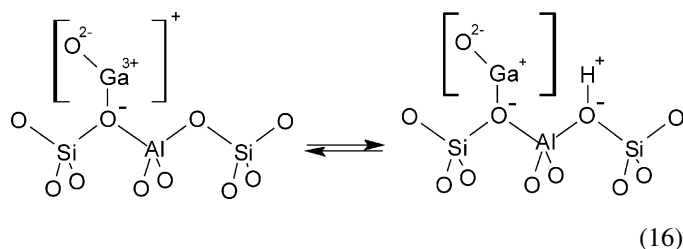
times more active than the tetrahedral framework Ga species. A complete inactivity of the tetrahedral Ga species has even been suggested [159].

Therefore, after calcination, most of the synthesized Ga/HMFI catalysts can be considered as mixtures of Ga_2O_3 and HMFI. However, these mixtures are not the real aromatization catalysts for significant changes in the nature and location of the Ga species as well as in the zeolite acidity were shown to occur during pretreatment with hydrogen or during propane aromatization (because of hydrogen production) at 500°C . These changes can have a significant beneficial effect on the aromatization activity and selectivity. However, the intimacy of Ga_2O_3 and HMFI is of paramount importance. Thus, with catalysts prepared by gentle mixture of Ga_2O_3 and HMFI the increase in activity is not substantial [150], whereas with highly intimate mixtures a significant increase can be observed [161].

The origin of this increase was first investigated by Kanizarev, Price and colleagues using gravimetric, DRX and FT-IR techniques [143–145,158,161,162]. Reduction was shown to occur during hydrogen treatment at high temperatures by a sequence of steps involving the formation of Ga_2O species which can migrate into the zeolite channels and undergo solid-state exchange with the zeolite protonic sites (Eqs. (14) and (15)).



This reduction was confirmed by the shift in Ga *K*-edge energy to lower values detected by in situ X-ray absorption measurements [142]. These measurements also shown that the reduced Ga species consisted of monomeric Ga^0 or Ga^+ compounds and that the reoxidation of reduced species to Ga^{3+} species occurred upon cooling to room temperature even in H_2 or propane [161]. Therefore, the active form of Ga species can be detected only at reaction conditions. Biscardi and Iglesia [43] suggest that the neutral $[\text{GaOH}]$ species stabilized by interaction with basic oxygens within MFI channels are the steady state form of reduced Ga (Eq. (16)).

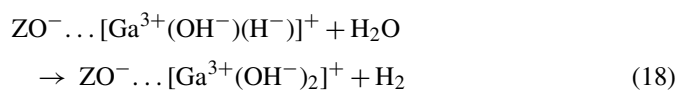


In agreement with reaction (15), H_2 treatment at high temperatures of Ga/HMFI samples causes a very significant decrease in the intensity of the bridging OH band at 3610 cm^{-1} [185]. However, a more limited decrease in the activity for model acidic reactions was observed: decrease by 1.5-times of the activity for *m*-xylene isomerization, by 1.4–2 times of that for propane transformation into methane [131,132] and by 1.4–1.6 times of the activity for 2-methyl-2-pentene isomerization [43]. This discrepancy could be due to reoxidation of reduced Ga

species upon cooling of the catalyst to room temperature for IR measurements.

However, this reoxidation cannot occur when all the protonic sites are exchanged by Ga^+ [127]. The corresponding Ga/MFI catalyst which has no measurable protonic acidity has a low activity for propane aromatization. Contrary to what is often observed over Ga/HMFI catalysts, aromatics are secondarily formed, which means that aromatization is limited by propene transformation (and not by propane dehydrogenation). A monofunctional mechanism was proposed to explain this aromatization in the apparent absence of protonic sites [127]. It could however be noted that an undetectable amount of protonic sites could be responsible for the very facile (at the high reaction temperatures) oligomerization and cyclization steps involved in bifunctional aromatization.

More recently, a DRIFT study of the nature of gallium species in GaMFI samples prepared by incipient wetness impregnation or via anchoring of trimethylgallium was carried out [152]. Reduction of the samples in hydrogen and evacuation at high temperature resulted in quantitative replacement of the protonic sites by Ga^+ ions. Ga^+ ions were shown to be partially oxidized by water at 300 °C with release of H_2 . After evacuation at 300 °C and cooling to room temperature a partial regeneration of protonic sites was also observed (regeneration of the bridging OH band at 3610 cm^{-1}). The following reactions (Eqs. (17)–(19)) were proposed to explain these observations:



Oxidative addition of hydrogen to Ga^+ at 500 °C resulted in the formation of stable gallium dihydride species. However, the authors conclude [152] that under typical aromatization conditions monovalent Ga^+ species are predominant even if $(\text{GaH}_2)^+$ species are also present. These species would be the active species able through an oxidative process to dissociate ethane into C_2H_5^- and H^- species as was the case for H_2 .

3.1.5. Comparison of Zn and of Ga/MFI catalysts

The aromatization of small alkanes was also investigated over MFI zeolites doped with various other agents: Pt [82,163–166], Zn [167–179], Cu [180], Ag [4], Ge [181], Re [182], Mo [183], Te [140]. A particular attention was placed on Zn/HMFI catalysts both from a fundamental and an applied point of view.

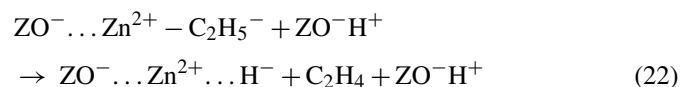
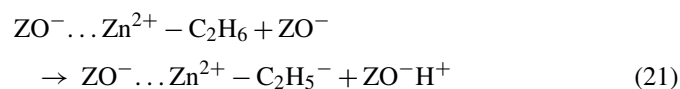
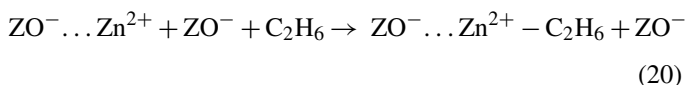
Depending on the authors and on the alkane reactant, Zn/HMFI catalysts were found more, or less performant (active and selective) in aromatization than Ga/HMFI catalysts. Note however that under the severe conditions of alkane aromatisation, Zn^0 can be formed by reduction with H_2 or hydrocarbons and eluted from the catalyst, which constitutes a serious drawback for the industrial use of Zn/HMFI catalysts [184].

Like with Ga/HMFI catalysts, it seems clear that aromatization of small alkanes occur through the bifunctional catalysis

pathway presented in Fig. 9 which involves successively dehydrogenating steps (steps 1, 5, 9 and 10) over Zn-containing species and oligomerization (step 3) and cyclization (step 7) steps over the protonic zeolite sites. Also like with Ga/HMFI catalysts, despite significant advances, the nature of the dehydrogenating species and the dehydrogenation mechanism are not perfectly established.

Like Ga/HMFI catalysts, Zn/HMFI catalysts can be prepared by various ways: ion exchange, impregnation, mechanical mixture of ZnO and of the zeolite [4], deposition of Zn vapor [177,178]. Different types of Zn species can be obtained. Thus, by impregnation of a HMFI zeolite (Si/Al=35) with an aqueous solution of $\text{Zn}(\text{NO}_3)_2$, drying then calcination at 550 °C for 12h, the resulting Zn/HMFI sample (8 wt.% Zn) was shown by CO adsorption to contain large ZnO crystals likely on the external surface, small ZnO clusters inside the micropores and Zn cations. Despite the large amount of Zn in the sample only part of the bridging OH groups were found to be exchanged [179]. In contrast, zinc vapor deposition at 500 °C can lead to a complete exchange of the zeolite protonic sites [178]. This difference seems to have consequences on alkane activation, this activation occurring essentially on the ZnO species with the first type of sample (8 wt.% Zn impregnated HMFI) [179] and on acid–base pairs (exchanged Zn^{2+} cations–framework oxygen atoms) with the second [178].

Large differences were shown between the modes of ethane activation over Ga^+ and Zn^{2+} in exchange position in MFI samples (without protonic sites) deduced from diffuse reflectance infrared spectroscopy (DRIFT) experiments. The mode of activation over Ga^+ has been described above: at relatively high temperature (250 °C), ethane activation would occur via oxidative addition with formation of ethyl and hydride fragments grafted to gallium (Eq. (11)) which decompose under prolonged heating into ethylene and gallium dihydrides (Eq. (12)). In the Zn/MFI samples, the positive charge of the Zn^{2+} cations is only partially compensated, hence these cations can be considered as Lewis superacids. At room temperature, ethane adsorbed over Zn^{2+} as shown in particular by the appearance of a band at 2738 cm^{-1} . Heating at 150 °C in an ethane atmosphere caused a decrease in the intensity of this band and a partial regeneration of the band corresponding to bridging OH groups (at 3610 cm^{-1}). After ethane evacuation at room temperature, three new bands in the region of the C–H stretching vibrations were visible. Heating at 250 °C led to the appearance of a band at 1934 cm^{-1} ascribed to zinc hydride. The following scheme was proposed to account for these observations (Eqs. (20)–(22)).



As a consequence of the regeneration of protonic acid sites, ethane aromatization took place over Zn/MFI, whereas only ethene formation occurred on Ga/MFI [178].

3.1.6. Conclusion

The commercial interest of LPG aromatization is well demonstrated with the development of several processes. The major interest of these processes is to allow the conversion of low value gaseous alkanes produced in remote fields into valuable and easier to be transported benzenic hydrocarbons.

The bifunctional character of the aromatization pathway with successive intervention of species containing Ga, Zn, etc. for dehydrogenation steps and of acidic protonic sites for oligomerization and cyclization steps is now well admitted. In contrast, despite the large number of studies devoted to aromatization (~500 papers) leaning on a large variety of techniques including the most advanced ones, both the exact nature of the dehydrogenating species and the dehydrogenation mechanism are not perfectly clarified. This is essentially due to the large differences in composition of the Ga (or Zn/MFI) samples which were used in the investigations: presence of different Ga (or Zn) species with different adsorption and catalytic properties, very low (~zero) to high concentration of protonic sites, etc., as well as to the significant modifications of the catalysts which occur frequently under pre-treatment and reaction conditions. The very systematic approach with use of model catalysts with perfectly specified physicochemical characteristics which is now followed should lead in the near future to a thorough understanding of this complex catalytic system.

3.2. *n*-Butane hydroisomerization and dehydroisomerization

Both types of reactions present a large commercial interest. The first one is already used to produce isobutane which is employed such as for the production of a high octane gasoline cut by aliphatic alkylation or is dehydrogenated into isobutene which has various applications: production of polymers, of methyltertiobutylether (MTBE), etc. [8]. The second one which combines in the same operation *n*-butane dehydrogenation with *n*-butene isomerization (one pot two-step reaction) constitutes a commercially (and conceptually) interesting alternative for isobutene synthesis [12].

3.2.1. Hydroisomerization of *n*-butane

It is well known that the stability of acidic zeolites can be significantly enhanced by noble metals such as Pt (or Pd), provided however that the reaction is carried out under hydrogen. Pt can play two roles depending on the strength of the acidic sites and on the reaction temperature [8,130,186]:

- When the acidity is strong enough so that the catalyst is active at low temperatures (e.g. highly chlorinated alumina, $\geq 150^\circ\text{C}$), the only role of Pt is to enhance the stability by activating hydrogen; the activated hydrogen reacts with carbenium ions limiting their concentration, hence, the formation of carbonaceous compounds responsible for deactivation [8,130,186].

- When, because of the too weak acidity of the catalyst, the reaction has to be carried out at high temperatures (e.g. silica–alumina, $>350^\circ\text{C}$), Pt additives play two roles: stabilization of the activity like with the strongly acidic catalysts but also development of a predominant bifunctional pathway involving successive chemical and diffusion steps, e.g. in *n*-alkane hydroisomerization: dehydrogenation of *n*-alkane into the corresponding alkenes over Pt sites, diffusion of these alkenes from the Pt to the protonic sites, isomerization of these alkenes into isoalkenes, diffusion of isoalkenes from the protonic sites to the Pt sites and then hydrogenation of these isoalkenes into isoalkanes [126]. As the reaction is carried out under hydrogen, olefinic intermediates are present in very low amounts [8,126,130]. This bifunctional scheme does not appear over the strongly acidic catalysts because firstly the acidic reaction is fast and secondly the amount of olefinic intermediates is too small at the low operating temperature.
- With sulphated zirconia and HMOR catalysts whose acid strength is intermediate between those of chlorinated alumina and silica–alumina, *n*-butane isomerization has to be carried out at intermediate temperatures (250°C) with possibility of conjunct participation of purely acidic and bifunctional pathways [8].

It should be remarked that with both the acidic and bifunctional mechanisms, the reaction order with respect to hydrogen will be negative, the increase in hydrogen pressure causing a decrease in the concentration of carbenium ion transition states.

A detailed comparison of *n*-butane transformation over HMOR and Pt/HMOR catalysts was reported in references [187,188]. Under hydrogen at 250°C , Pt causes a significant improvement in stability but a very important decrease in activity especially for the formation of isobutane and pentanes; moreover, hydrogenolysis products (methane, ethane, etc.) appear in large amounts. Operating at higher temperatures causes, in addition to the expected increase in activity, a significant increase in the selectivity to isobutane. However, at these high temperatures ($>350^\circ\text{C}$), *n*-butane isomerization occurs most likely through the bifunctional pathway. Indeed the apparent activation energy is much higher than for an acid mechanism: $90\text{--}110\text{ kJ mol}^{-1}$ [75] against $35\text{--}40\text{ kJ mol}^{-1}$ on chlorinated alumina [8]. Furthermore, there are no definite arguments in the literature in favour of a bimolecular or of a monomolecular mode of *n*-butane isomerization.

Mesopores were shown to have a positive effect on the selectivity to isobutane of bifunctional Pd mordenite catalysts [189,190]. The location of the noble metals plays a significant role. As the introduction through ion exchange could lead to a partial blockage of the HMOR channels, the best method of catalyst preparation seems to be through intimate physical mixing of the acidic component (HMOR) and of Pt or Pd dispersed on a support such as montmorillonite (the so-called hybrid catalysts). Compared to supported Pd/HMOR, hybrid catalysts were shown to be more selective to isobutane, an additional advantage for their industrial use being their mechanical resistance against attrition [191].

n-Butane transformation was also investigated on Pd or Pt supported on other acidic zeolites: HMFI [189,192–194], HBEA [193], HTON [74] and HFER [74], but generally at temperatures ≥ 350 °C. Whatever the zeolite component, a high selectivity to isobutane (60–90%) can be obtained but only at relatively low conversions (<30%). However, at these operating temperatures, the percentage at thermodynamic equilibrium of isobutane in the *n*-butane/isobutane mixture is lower than 40%, which makes non-economical the industrial development of these catalysts. Liu et al. [195] questioned the low activity of HMOR compared to sulphated zirconia catalysts which have nevertheless similar acid strength. According to these authors this difference would be due to the geometrical constraints exerted by the one-dimensional channels in MOR on the dimerization step of the bimolecular mechanism.

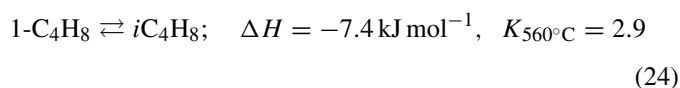
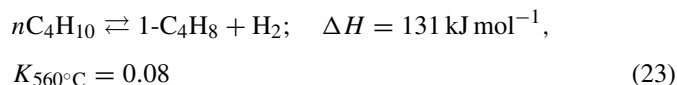
3.2.2. Dehydroisomerization of *n*-butane

Two different concepts have been followed to transform in the same reactor *n*-butane into isobutene: use of either two different catalysts in successive beds, the first one active in dehydrogenation the second one in butene isomerization or of a bifunctional system constituted of only one catalyst or resulting from physical mixture of two catalysts with dehydrogenation and isomerization functions.

An example of the two-bed system is the one presented by Bellussi et al. [196]: the first bed is constituted of a Pt/silylated alumina promoted with In and Sn (*n*-butane dehydrogenation) the second one of Boralite (butene isomerization). In another example, Pd/HMFI was used in the first bed, HMCM22 in the second [197].

The bifunctional systems which were tested contained generally zeolites. It is the case for the mixture of dehydrogenating and isomerization components, e.g. Cr₂O₃ + MFI metallosilicates [198], Zn/K-HMFI + TON [199] as well as for the purely bifunctional catalysts, essentially Pt (alone or associated with Mn, Cu, Sn) supported on large pore zeolites: MOR [200], FAU [201]; average pore zeolites: MEL [202], MFI [12,203,204], FER [204], TON [204,205], MWW [197] or on aluminophosphates [206]. *n*-Butane dehydroisomerization was also investigated over Ga/SAPO11 [207].

Eqs. (23) and (24) show that dehydroisomerization is a combination of an endothermic reaction (dehydrogenation) hence thermodynamically favoured at high temperatures and of a slightly exothermic reaction (butene isomerization) favoured at low temperatures.



Both equilibria limit the maximum yield in isobutene. Moreover, an additional reaction, the dehydrogenation of butene into butadiene which is a precursor of coke has to be considered for choosing the operating conditions [12]. Thus, hydrogen has to be

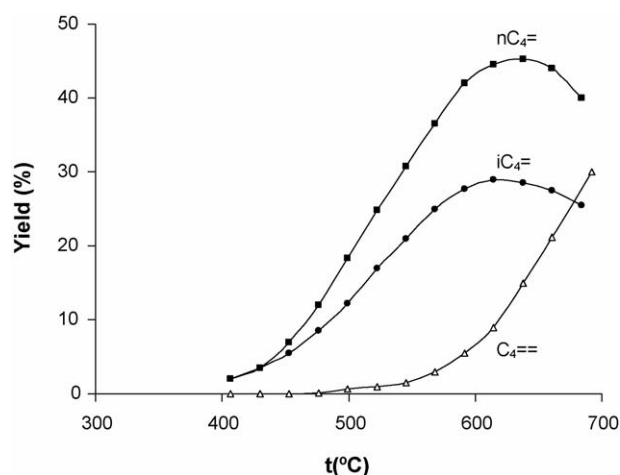


Fig. 11. Yields at thermodynamic equilibrium as a function of temperature. Feed composition: 10% *n*-butane, 20% H₂, 70% N₂, pressure of 1.8 bar.

added to the feed in order to limit deactivation by coking, which for a thermodynamic point of view is detrimental for butene formation. For the same reason, the operating temperature will be chosen low enough to limit butadiene formation, hence as shown in Fig. 11, it will be lower than the temperature corresponding to the maximum yield in isobutene [12].

3.2.2.1. Reaction scheme. The reaction scheme of *n*-butane dehydroisomerization was established over Pt/HMFI with high Si/Al ratios hence with low acid site concentrations, under the following conditions: 560 °C, $p_{\text{H}_2} = 0.36$ bar, $p_{n\text{-butane}} = 0.18$ bar [12]. Under these conditions, deactivation is relatively fast: decrease in activity of $\sim 30\%$ in 2.5 h. In addition to *n*-butene and isobutene, various by-products can be observed: methane, ethene, ethane, propene, propane, isobutane and pentenes. Butenes resulting from butane dehydrogenation were the main primary products (<95%). Furthermore, as shown by comparing the products obtained over Pt/HMFI and HMFI, butane undergoes two other primary reactions: protolytic cracking into methane + propene and ethane + ethene over the acidic sites of the zeolite and hydrogenolysis into methane, ethane and propane over the Pt sites. Whereas the first one plays always a minor role, the contribution of hydrogenolysis increases at high conversion when *n*-butane consumption through dehydrogenation approaches thermodynamic equilibrium.

n-Butene undergoes secondary reactions, in particular the formation of isobutene, propene and pentenes, which suggests *n*-butene transformation through an oligomerization–isomerization–cracking mechanism. Note again that this type of process leads always in parallel to propene + pentenes and to isobutene. The propene/pentenes molar ratio is much higher than 1 suggesting that oligomer intermediates are not only dimers. At the high reaction temperature these oligomers are very unfavored at thermodynamic equilibrium, hence cannot be observed in the reaction products. In addition to ethene, propene, isobutene, pentenes, the corresponding alkanes are also formed. The alkane/alkene ratio (ethane/ethene, etc.) increases

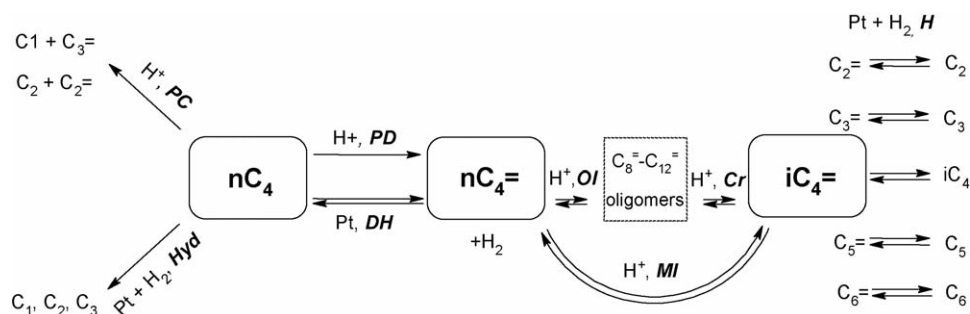


Fig. 12. Dehydroisomerization of *n*-butane over a bifunctional Pt/H zeolite catalyst. Bifunctional scheme. PC: protolytic cracking; Hyd: hydrogenolysis; PD: protolytic dehydrogenation; DH: dehydrogenation; OI: oligomerization; Cr: cracking; MI: monomolecular isomerization; H: hydrogenation.

with *n*-butane conversion, which indicates that alkanes result from alkene hydrogenation.

The reaction scheme of *n*-butane transformation over Pt/HMFI is represented in Fig. 12. As it was also demonstrated over (Pt/Cu)HTON catalysts [205], isobutene results from a bifunctional pathway involving successively butane dehydrogenation over the Pt sites then *n*-butene isomerization over the protonic sites. The alternative bifunctional scheme involving successively butane isomerization then isobutene dehydrogenation can be excluded. Indeed butenes which appear as primary products are much more reactive than isobutene which moreover is secondarily formed in relatively low amounts.

3.2.2.2. Influence of catalytic characteristics and operating conditions. The balance between hydrogenating and acid functions of Pt zeolite catalysts used in classical bifunctional reactions such as hydroisomerization and hydrocracking is known to determine for a large part the catalyst properties. This balance generally expressed as the ratio between the concentrations of accessible Pt and protonic sites (n_{Pt}/n_A) [208] was used by Pirmgruber et al. [12] in the case of butane dehydroisomerization over Pt/HMFI catalysts. Fig. 13a and b show that whatever *n*-

butane conversion, the higher n_{Pt}/n_A , the higher the selectivity to butenes (*n* + *iso*) and the lower the selectivity to the main by-products (ethane, propene, propane and pentenes).

The highest yield of isobutene was obtained over the sample with the highest value of n_{Pt}/n_A (0.34) which contains 0.5 wt.% Pt well dispersed on a Pt/HMFI sample with a Si/Al ratio of 240, hence with a very low concentration of protonic sites. This yield is of ~12%, the conversion of *n*-butane being of ~64%; *n*-butenes are practically in thermodynamic equilibrium with *n*-butane but the approach of the *n*-butene/isobutene equilibrium is of only 50%. A better approach of this equilibrium can be obtained by operating at higher conversions or with more acidic catalysts (lower n_{Pt}/n_A ratios) but at the expense of the selectivity to butenes (*n* + *iso*).

A kinetic study was carried out over the PtHMFI catalysts [203]. The main conclusions are summarized below:

1. High temperature and low pressures reduce the formation of by-products through the oligomerization–isomerization–cracking pathway and the thermodynamic constraints of dehydrogenation. However, above 560 °C these improvements are overcompensated by a loss in catalyst stability ascribed to poisoning of the Pt and acidic sites by butadiene

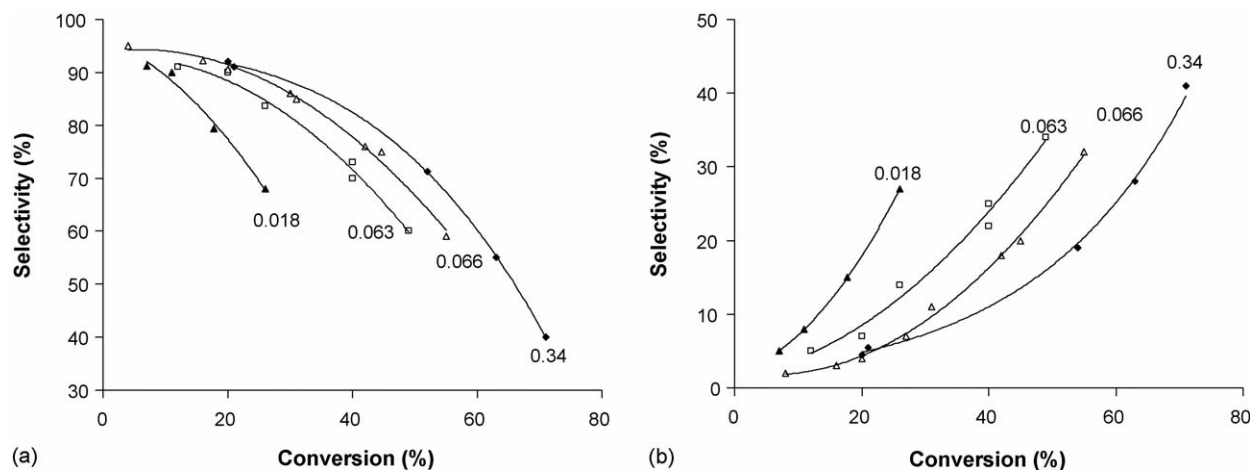


Fig. 13. Dehydroisomerization of *n*-butane over bifunctional Pt/HMFI catalysts. Effect on the selectivity of the balance between Pt and acidic functions (taken as the ratio between the concentrations of accessible Pt and protonic sites: from 0.018 to 0.34). (a) Selectivity to the sum of butenes. (b) Selectivity to the main by-products. From reference [12].

and by coke resulting from its transformation. The authors account for the decrease in by-products by an increase of the participation of the monomolecular mechanism in butene isomerization. Another explanation could be the reduction in size of oligomers to dimers which can lead selectively to isobutene [209].

2. The increase in the H_2/n -butane ratio causes an enhancement of the non-desired hydrogenolysis reactions without increasing significantly the catalyst stability. The optimum with respect to selectivity and stability was found for H_2/n -butane = 2.

As the main secondary products formed on Pt/HMFI result from cracking of butene oligomers, other zeolites: HFER, HTON, HMWW known as more selective than HMFI for n -butene isomerization were chosen for n -butane dehydroisomerization. Pt/HFER and Pt/HTON [204] were found to be less selective to isobutene than Pt/HMFI because of a more significant contribution of protolytic cracking and hydrogenolysis in the formation of secondary products. This low selectivity could be partly due to the low dehydrogenating activity of these Pt zeolites because of limitations to the access of small Pt particles located in the narrow micropores (low value of the n_{Pt}/n_A ratio). In contrast, at low temperatures (up to 500 °C), Pt/HMWW achieved higher yields of isobutene than Pt/HMFI catalysts [197]. The distribution of by-products was very different with less cracking products and more isobutane (formed by isobutene hydrogenation) than on Pt/HMFI. Unfortunately, especially at high temperatures, Pt/HMWW catalysts are not very stable, deactivation most likely by coking, affecting both the dehydrogenating and acidic sites. Note that the two-bed approach with the very efficient zeolite catalysts for butene isomerization (HFER, HMWW) in the second bed could be attractive. Slightly better results than on Pt/HMFI catalysts were furthermore obtained through this approach by using HMWW in combination with Pt/HMFI in the first bed acting mainly as a dehydrogenating catalyst.

The selectivity of n -butane dehydroisomerization could also be enhanced by limiting the secondary reaction of hydrogenolysis. This can be made by the classical way, i.e., by substituting bimetallic catalysts (Pt–Cu [205], Pt–In [201]) for Pt. Indeed hydrogenolysis is well known to be a structure sensitive reaction (i.e., which requires several adjacent Pt sites), which is not the case for hydrogenation/dehydrogenation reactions [210]. Therefore, the reduction of the size of the Pt ensembles by dilution with a second metal should cause an inhibition of hydrogenolysis reactions and an increase in the dehydrogenation selectivity. It is what was clearly observed by substituting Pt (supported on HFAU) by Pt–Sn: increase in the selectivity to n -butenes and isobutene at the expense of the selectivity to C_1 – C_3 alkanes [201].

n -Butane dehydroisomerization was also investigated over bifunctional catalysts based on MnAPO11 [206] and SAPO11 [207] hence with weak acid sites. The best results were obtained with Ga/SAPO11 at 500 °C with a dehydrogenation yield close to the thermodynamic limit and an approach to equilibrium of butene isomerization of ~70%.

3.2.2.3. Conclusion. Butane dehydroisomerization was demonstrated to occur over Pt/acid zeolites through two successive reactions: n -butane dehydrogenation over Pt sites then butene isomerization over protonic sites. The choice of operation conditions is determined by severe thermodynamic constraints: high temperatures are required for butane dehydrogenation into butenes but at too high temperatures (and too low hydrogen/ n -butane ratio), butadiene which is a coke maker molecule is formed in too large amounts. Moreover, butene isomerization is thermodynamically favoured at low temperatures. In addition to the operation conditions, the balance between the hydrogenation and acid functions and the pore structure of the zeolite are, as is it is generally the case with bifunctional catalysts, the parameters determining the yield in the desired product and the catalyst stability. Four main types of secondary reactions can be observed: protolytic cracking, hydrogenolysis on the Pt sites, cracking of butene oligomers and isobutene hydrogenation. Whereas all these reactions can be limited by optimizing the bifunctional catalyst and the operating conditions, the use of a two-bed reactor, the first one with a dehydrogenating catalyst, the second one with a selective butene isomerization catalyst seems to be the best solution (more flexibility, etc.) for a commercial process. However, additional work has to be carried out to obtain higher yields in isobutene (up to now of only ~15%).

3.3. Alkylation of aromatics with small alkanes

Environment-friendly zeolite catalysts have largely replaced Friedel Crafts catalysts in the commercially important processes of ethylbenzene, ethyltoluenes and cumene synthesis through benzene or toluene alkylation with ethene and propene. Since these alkenes can be selectively produced by dehydrogenation, a one pot alkylation of aromatics with small alkanes could be possible over bifunctional zeolite catalysts (Fig. 14). This possibility was explored over Pt or Pd and Ga H zeolites [13,14,211–222], the best results being always obtained with the tri-dimensional average pore size MFI zeolite. Large pore size zeolites such as FAU and MOR and average pore size zeolites with micropores smaller than those of MFI gave low conversion and/or poor selectivity.

3.3.1. Thermodynamic considerations

Fig. 15a and b show the equilibrium conversion for the transformation of an equimolar mixture of benzene and ethane or propane into the desired products: ethylbenzene or cumene. In the range of temperature chosen in the literature: 300–550 °C, the equilibrium conversion into ethylbenzene and into cumene increases from 11.5 to 26.7% and from 7.6 to 15.4%, respectively. Of course operating with a higher alkane/benzene molar ratio leads to higher equilibrium values. Thus, for the ratio of 4 chosen in reference [211], the equilibrium conversion into ethylbenzene increases from 22.7 to 44.8% from 300 to 550 °C and the one into cumene from 15 to 29.4%. Fig. 15a and b report also the equilibrium conversion for the formation of the main secondary products which were observed: toluene in alkylation of benzene with ethane

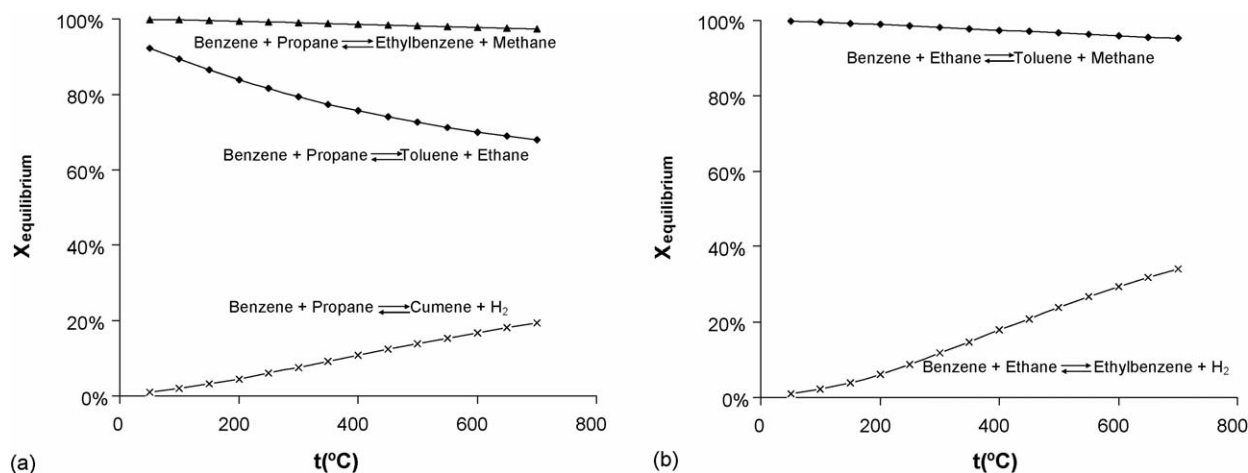


Fig. 14. Conversion X at thermodynamic equilibrium vs. temperature. (a) Transformation of the equimolar mixture of benzene and ethane into ethylbenzene and H₂ or into toluene and methane. (b) Transformation of the equimolar mixture of benzene and propane into cumene + H₂, into ethylbenzene and methane or into toluene and methane.

and, propane and ethylbenzene in alkylation of benzene with propane.

3.3.2. Alkylation over Pt or Pd/HMFI catalysts

The products expected from alkylation, i.e., ethylbenzene, ethyltoluenes or cumene are formed over Pt or Pd/HMFI catalysts. Under identical operating conditions, the activity of mixtures of Pt/non-acidic support and HMFI is much higher than those of the components, as could be expected from a bifunctional mechanism [126,130]; Pt/HMFI catalysts on which Pt and protonic sites are closer are more active than the physical mixture in which alkylation is likely limited by the migration step of alkene intermediates from the Pt sites to the acidic sites (step M in Fig. 14).

In toluene alkylation with ethane, the optimum yield to ethyltoluenes over a 0.9 wt.% Pd/HMFI(25) catalyst (Si/Al = 25) was found at 350 °C and with an ethane/toluene molar ratio of 4 [211]. At higher temperatures and for ratios smaller than 4, the selectivity to ethyltoluenes was lower, whereas at lower temperatures the activity was too low. A significant initial decrease in toluene conversion can be observed followed by a quasi plateau in activity after 400 min time-on stream. The activity decrease is essentially due to the disappearance of the products of toluene disproportionation (benzene and xylenes) over the zeolite acid

sites with therefore a significant increase of the selectivity to ethyltoluenes: from 25 to 80% and practically no change in the yield in ethyltoluenes. It should be remarked that under the operating conditions no ethene was observed in the reaction products, which suggests that ethyltoluene formation was kinetically limited by ethane dehydrogenation (step D in Fig. 14).

In contrast, a large amount of ethene (~twice the one of ethylbenzene) was observed in the products of benzene alkylation with ethane at 500 °C, ethane/benzene molar ratio of 5 over a Pt/HMFI catalyst with a very large amount of Pt (6.8 wt.%) [13,213]. Therefore, the alkylation (step A in Fig. 15) could be the limiting step of the bifunctional scheme. However, as the rate of ethylbenzene formation is practically independent on the Si/Al ratio of the HMFI zeolite, hence on the acid site concentration, that cannot be the case. Thermodynamic equilibrium of the A step which is largely in favour of dealkylation at the high reaction temperature could be responsible for this large amount of ethene in the products.

The maximum yields in ethylbenzene and ethyltoluenes which were reported in these preliminary experiments are not very high: 7.3 and 1.4 wt.% based on benzene and toluene respectively, which corresponds to ~40% of the equilibrium value. Note also that while the paper on toluene ethylation is well documented with respect to selectivity and stability [211],

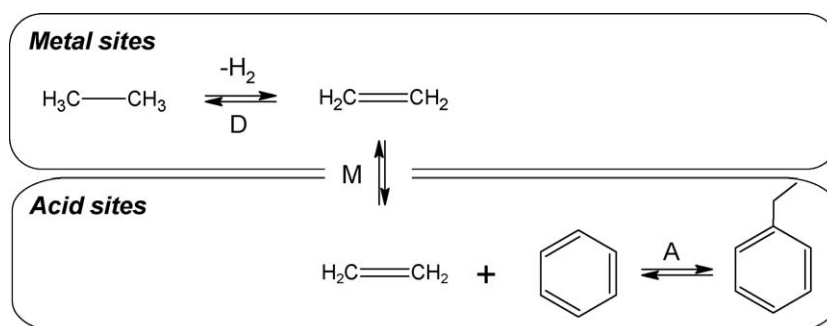


Fig. 15. Alkylation of benzene with ethane over a bifunctional Metal/H zeolite catalyst. Bifunctional scheme. D: dehydrogenation; M: migration of ethene from the metal to the acid sites; A: alkylation of benzene with ethene.

Table 3

Benzene alkylation with propane over HMFI, 0.2–0.3 wt.% Pt/HMFI catalysts and effect of a H₂ scavenger (Zr₂Fe) [14]

X _p	0.86	6.62	44.56	14.36
	HMFI (50)	Pt/HMFI (150)	Pt/HMFI (25)	Pt/HMFI (150) + Zr ₂ Fe
Selectivity (mol.%)				
CH ₄	20.36	0.38	4.39	0.24
C ₂ H ₆	0.99	4.91	27.83	3.69
C ₃ H ₆	1.22	13.62	0.35	12.31
C ₄ –C ₅	2.88	6.85	10.26	11.83
T	15.17	1.27	19.58	1.04
EB	35.12	0.88	1.37	1.18
IPB	5.79	23.28	1.58	23.11
NPB	10.04	36.60	3.24	35.65
C ₉ –C ₁₁	–	3.86	7.73	8.63
Others	8.03	8.35	23.67	2.32

nothing is said on these essential features in the case of benzene ethylation [213].

Benzene alkylation with propane over 0.2–0.3 wt.% Pt/HMFI at 350 °C [14] leads to a larger diversity of products (Table 3) than toluene ethylation. Indeed, over Pt/HMFI samples with Si/Al ratios of 150, 50 and 25 and a propane/benzene ratio of 1, there is in addition to the expected propylbenzene products (cumene IPB and *n*-propylbenzene NPB) formation of toluene, ethylbenzene, C₉–C₁₁ alkylbenzenes, methane, ethane, C₄–C₅ hydrocarbons. Propene can also be observed, the selectivity to this product decreasing with the zeolite Si/Al ratio, hence with the increase in acid site concentration: from 13.6% for Si/Al = 150 to 0.35% for Si/Al = 25 (Table 3). Propane conversion increases with decreasing Si/Al: 6.6% for Si/Al = 150 to 44.6% for Si/Al = 25 (Table 3). It is almost proportional to the acid site concentration, which suggests that the limiting step of propane transformation (and product formation) is catalyzed by the zeolite protonic sites. A significant change in the product distribution can also be observed with a significant decrease with the Si/Al ratio in propylbenzenes at the benefit of toluene, methane, ethane and C₄–C₅; however, this change in selectivity seems to be more related to the increase in conversion (hence in the secondary transformations of propylbenzenes) than to the increase in the acid site density. It should be noticed that the same products were formed but much more slowly on the pure HMFI samples. The addition to Pt/HMFI of an H₂ scavenger (a Zr₂Fe intermetallic compound) to shift the thermodynamic equilibrium of benzene alkylation with propane causes an increase in propane conversion but no significant change in the product distribution. The highest propylbenzene production was obtained with the association of Pt/HMFI(150) and Zr₂Fe: yield of 8.5% with a selectivity of ~60% (Table 3) and with a good catalyst stability (however, limited by the saturation of the H₂ scavenger).

The product distribution and its change with the characteristics of the catalyst can be explained by the scheme presented in Fig. 16. Benzene adsorbs on the protonic sites of the zeolite with formation of benzenium ions. Hydride transfer to these cations leads to cyclohexadiene and isopropyl carbenium ions (step 1). These cations can also result from two other ways:

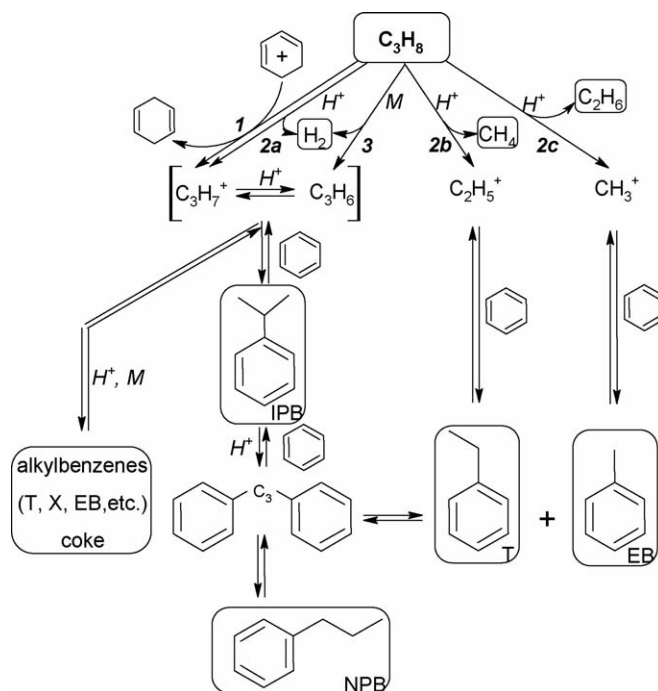


Fig. 16. Steps involved in benzene alkylation with propane over bifunctional M/HMFI catalysts. M = Pt, Pd, Ga, etc. Step 1: hydride transfer from propane molecules to benzenium ions; step 2: protolytic dehydrogenation (a) or cracking (b, c); step 3: propane dehydrogenation on the metal sites. The other steps deal with purely acidic transformations: benzene alkylation into cumene, ethylbenzene and toluene, bimolecular isomerization of cumene into *n*-propylbenzene or disproportionation into toluene + ethylbenzene and topropene and with the bifunctional aromatization of propene.

protolytic dehydrogenation of propane (step 2a) and protonation of propene resulting from propane dehydrogenation over the Pt sites (step 3). The isopropyl carbenium ions can either alkylate benzene into cumene or be transformed into aromatics. Propane can also undergo protolytic cracking (steps 2b and c) leading to ethane or methane plus methyl or ethyl carbenium ions which alkylate benzene into toluene or ethylbenzene. Toluene and ethylbenzene could also result from cracking of the diphenyl propane intermediates of cumene isomerization into *n*-propylbenzene. It should be emphasized that cumene formation is thermodynamically limited, hence that the reverse step (dealkylation) can play a significant role at high propane conversion, with formation of a significant amount of propene which can be transformed into benzenic hydrocarbons.

3.3.3. Alkylation over Ga/HMFI catalysts

Alkylation of benzene with propane was also investigated over Ga/HMFI catalysts, the reaction being carried out under static conditions using ¹³C-NMR [218,219] or FT-IR [220] to specify the reaction mechanisms or under more realistic flow conditions [221,222]. In the initial stage of the reaction, major resonances corresponding to toluene, ethylbenzene, ethane and methane with weak resonances assigned to cyclohexadiene, cumene and *n*-propylbenzene are shown in ¹³C-NMR spectra [218]. Afterwards, the lines corresponding to cyclohexadiene and cumene disappear then those of ethylbenzene and *n*-propylbenzene, whereas those corresponding to toluene and

methane become predominant. Experiments were also carried out with cumene in presence of benzene in order to confirm the possible formation of toluene and ethylbenzene from the diphenyl propane intermediates of cumene isomerization [218]. The results obtained lead the authors to consider this mode of formation as minor and to propose that toluene and ethylbenzene result essentially from direct benzene alkylation with methyl and ethyl carbenium ions. The same conclusion was advanced to explain the significant formation of toluene and ethylbenzene observed in flow reactor over a Ga/HMFI catalyst [222]. However, it should be remarked that this conclusion is not in agreement with the well-known much higher selectivity of Ga/HMFI for dehydrogenation compared to cracking [131]. Therefore, it is most likely that a large part of toluene, ethylbenzene and other aromatics result simply from propene aromatization. The apparent secondary transformation of propylbenzenes would be thus due to their dealkylation followed by propene aromatization.

3.3.4. Conclusion

Alkylation of benzene (or toluene) with ethane and propane was shown to be feasible in one apparent step using Pt, Pd and Ga/HMFI catalysts. A reaction scheme was proposed to account for the formation of the desired products: ethylbenzene, cumene, etc. and of secondary products formed in large amounts, especially in alkylation with propane. These secondary reactions as well as the severe thermodynamic constraints have a very negative effect on the production of the desired products. However, the two-bed reactor system with the first bed constituted by a non-acidic selective dehydrogenation catalyst, the second one by an alkylation catalyst could bring, like in *n*-butane dehydroisomerization, a significant improvement.

4. General conclusion

This review paper, although limited to non-oxidative transformations of C₂–C₄ alkanes on zeolite catalysts, demonstrates the large interest of the scientific community for the great challenge that constitutes the substitution of these cheap and readily available hydrocarbons for the very reactive but expansive light alkenes. The most significant advances of the last decade deal with the fundamental aspects, the nature of the active sites and their mode of action being now well clarified:

- 1- Alkane activation on strong protonic sites of zeolites by protolytic dehydrogenation and cracking is now well-admitted, even if some observations are not completely understood.
- 2- The composition of the carbonaceous deposits (“coke”) responsible for the deactivation of zeolite catalysts used in isobutane–butene alkylation was established. This allowed the development of milder modes for “coke” removal, which has as benefit a complete restoration of the initial activity of the not very stable catalysts.
- 3- The bifunctional character of the aromatization pathway with successive intervention of species containing Ga for dehydrogenation steps and of acidic sites for oligomerisation and cyclisation steps is now well admitted. The dehydrogenation

steps involve bifunctional sites associating neighbouring Ga species (most likely Ga⁺) and protonic sites.

- 4- One pot two-step transformations into valuable products such as isobutene and alkylbenzenes were shown to be feasible over bifunctional zeolite catalysts. Thus, alkylation of benzenic hydrocarbons with light alkanes occurs in one apparent step over bifunctional Pt, Pd and Ga/HMFI catalysts. Furthermore, *n*-butane dehydroisomerisation was demonstrated to occur through *n*-butane dehydrogenation over Pt sites followed by isomerisation of *n*-butene into isobutene over the zeolite acid sites. In both cases the main problem to solve deals with the too low selectivity to the desired products.

Some of the fundamental advances could open the route to the development of new and greener commercial processes. Processes have already been developed for LPG aromatisation. These processes present a large interest for the conversion of the low value light alkanes produced in remote fields into valuable and easier to be transported BTX hydrocarbons and into hydrogen which can be used on site. The significant advances made in isobutane–butene alkylation both in the lifetime of zeolite catalysts and in their regeneration could lead to the substitution of sulphuric and hydrofluoric acids by these environment-friendly catalysts. Lastly, the preliminary experiments which were carried out show that bifunctional zeolite catalysts can catalyse, in one apparent step, alkane transformations which require two successive steps, avoiding polluting and costly separation steps. However, additional work is indispensable to make the catalysts enough stable and selective for an industrial development.

Acknowledgements

M.G. acknowledges the Gulbenkian Foundation for a grant as Invited Professor at IST, Universidade Técnica de Lisboa, G.C. and R.H.C. the PhD grants (BD/13411/2003 POCI 2010 and BD/13416/2003 POCI 2010) from Fundação para a Ciência e Tecnologia (FCT).

References

- [1] E.G. Derouane, J. Haber, F. Lemos, F. Ramôa Ribeiro, M. Guisnet (Eds.) Catalytic Activation and Functionalisation of Light Alkanes, NATO ASI series III, vol. 44, 1997.
- [2] E.G. Derouane, V. Parmon, F. Lemos, F. Ramôa Ribeiro (Eds.), Sustainable Strategies for the Upgrading of Natural Gas: Fundamentals, Challenges, and Opportunities, NATO Science series II, vol. 191, 1995.
- [3] M. Guisnet, N.S. Gnep, F. Alario, Appl. Catal. A: Gen. 89 (1992) 1.
- [4] Y. Ono, Catal. Rev. -Sci. Eng. 34 (1992) 179.
- [5] G. Giannetto, R. Monque, R. Galiasso, Catal. Rev. -Sci. Eng. 36 (1994) 271.
- [6] K.M. Dooley, G.L. Price, Catal. Today 31 (1996) 189.
- [7] M. Guisnet, N.S. Gnep, Appl. Catal. A: Gen. 146 (1996) 33.
- [8] C. Marcilly, Catalyse acido-basique. Application au raffinage et à la pétrochimie. Editions Technip, Paris, 2005.
- [9] J. Pérez-Ramírez, E.V. Kondratenko, Chem. Commun. (2003) 382.
- [10] J. Pérez-Ramírez, A. Gallardo Llamas, J. Catal. 223 (2004) 382.
- [11] J. Pérez-Ramírez, A. Gallardo Llamas, Appl. Catal. A: Gen. 279 (2005) 117.
- [12] G.D. Pirngruber, K. Seshan, J.A. Lercher, J. Catal. 186 (1999) 188.

- [13] S. Kato, K. Nakagawa, N.-O. Ikenaga, T. Suzuki, *Chem. Lett.* (1999) 207.
- [14] A.V. Smirnov, E.V. Mazina, V.V. Yuschenko, E.E. Knyazeva, S.N. Nesterenko, I.I. Ivanova, L. Galperin, R. Jensen, S. Bradley, *J. Catal.* 194 (2000) 266.
- [15] J. Weitkamp, P.A. Jacobs, J.A. Martens, *Appl. Catal.* 8 (1983) 123.
- [16] V.B. Kazansky, I.N. Senchenya, *J. Catal.* 119 (1989) 108.
- [17] I.N. Senchenya, V.B. Kazansky, *Catal. Lett.* 8 (1991) 317.
- [18] V.B. Kazansky, M.V. Frash, R.A. van Santen, *Catal. Lett.* 48 (1997) 61.
- [19] B. Aditya, V. Yogesh, W. Joshi, N. Delgass, K.T. Thomson, *J. Phys. Chem. B* 107 (2003) 10476.
- [20] V.B. Kazansky, *Catal. Today* 51 (1999) 419.
- [21] M.V. Frash, V.B. Kazansky, A.M. Rigby, R.A. van Santen, *J. Phys. Chem. B* 102 (1998) 2232.
- [22] A.M. Rigby, G.J. Kramer, R.A. van Santen, *J. Catal.* 170 (1997) 1.
- [23] S.R. Blaszowski, R.A. van Santen, *Top. Catal.* 4 (1997) 145.
- [24] M. Boronat, P. Viruela, A. Corma, *J. Phys. Chem. A* 102 (1998) 982.
- [25] M. Boronat, P. Viruela, A. Corma, *PCCP* 3 (2001) 3235.
- [26] A. Corma, A.V. Orchillés, *Microp. Mesop. Mat.* 35–36 (2000) 21.
- [27] W.O. Haag, R.M. Dessau, *Proceedings of the 8th International Congress of Catalysis, Frankfurt-am-Main, 1984*, p. 305.
- [28] G.A. Olah, P. Schilling, J.S. Staral, Y. Halpern, J.A. Olah, *J. Am. Chem. Soc.* 97 (1975) 6807.
- [29] J. Bandiera, Y.B. Taarit, *Appl. Catal. A: Gen.* 2 (1990) 309.
- [30] R. Shigeishi, A. Garforth, I. Harris, J. Dwyer, *J. Catal.* 130 (1991) 423.
- [31] M. Guisnet, N.S. Gnep, D. Aittaleb, Y.J. Doyemet, *Appl. Catal. A: Gen.* 87 (1992) 255.
- [32] H. Kranilla, W.O. Haag, B.C. Gates, *J. Catal.* 135 (1992) 115.
- [33] A. Corma, V. González-Alfaro, A.V. Orchillés, *Appl. Catal. A: Gen.* 187 (1999) 245.
- [34] A.F.H. Wielers, M. Vaarkamp, M.F.M. Post, *J. Catal.* 127 (1991) 51.
- [35] C. Mirodatos, D. Barthomeuf, *J. Catal.* 114 (1989) 121.
- [36] J.P. Marques, I. Gener, J.M. Lopes, F. Ramôa Ribeiro, M. Guisnet, *Catal. Today* 107–108 (2005) 726.
- [37] L.A. Pine, P.J. Maher, W.A. Watcher, *J. Catal.* 85 (1984) 466.
- [38] G. Giannetto, S. Sansare, M. Guisnet, *J. Chem. Soc.- Chem. Commun.* (1986) 1303.
- [39] A.W. Peters, W.C. Cheng, M. Shatlock, R.F. Wormsbecker, E.T. Habib, in: D. Barthomeuf, et al. (Eds.), *Guidelines for Mastering the Properties of Molecular Sieves*, NATO ASI, series B, vol. 221 Plenum Press, 1990, p. 365.
- [40] E. Jacquino, A. Mendes, F. Raatz, C. Marcilly, F.R. Ribeiro, J. Caeiro, *Appl. Catal.* 60 (1990) 101.
- [41] J.A. Lercher, R.A. van Santen, H. Vinek, *Catal. Lett.* 27 (1994) 91.
- [42] T.F. Narbeshuber, M. Stockenhuber, A. Brait, K. Seshan, J.A. Lercher, *J. Catal.* 160 (1996) 183.
- [43] J.A. Biscardi, E. Iglesia, *Catal. Today* 31 (1996) 207.
- [44] J.A. Biscardi, E. Iglesia, *J. Catal.* 82 (1999) 117.
- [45] N. Essayem, G. Coudurier, J.C. Vedrine, D. Habermacher, J. Sommer, *J. Catal.* 183 (1999) 292.
- [46] W. Hua, A. Sassi, A. Goepfert, F. Taulelle, C. Lorentz, J. Sommer, *J. Catal.* 204 (2001) 460.
- [47] M. Haouas, S. Walspurger, J. Sommer, *J. Catal.* 215 (2003) 122.
- [48] I.I. Ivanova, E.B. Pomakhina, A.I. Rebrov, E.G. Derouane, *Top. Catal.* 6 (1998) 49.
- [49] G.J. Kramer, R.A. van Santen, C.A. Emeis, A.K. Nowak, *Nature* 363 (1993) 529.
- [50] V.B. Kazansky, M.V. Frash, R.A. van Santen, *Catal. Lett.* 28 (1994) 211.
- [51] V.B. Kazansky, I.N. Senchenya, M. Frash, R.A. van Santen, *Catal. Lett.* 7 (1994) 345.
- [52] S.J. Collins, P.J. O'Malley, *Chem. Phys. Lett.* 28 (1994) 246.
- [53] S.J. Collins, P.J. O'Malley, *Chem. Phys. Lett.* 246 (1995) 555.
- [54] S.J. Collins, P.J. O'Malley, *J. Catal.* 53 (1995) 94.
- [55] S.A. Zymunt, L.A. Curtiss, P. Zapol, L.E. Iton, *J. Phys. Chem. B* 104 (2000) 1944.
- [56] X. Zheng, P. Blowers, *J. Mol. Catal. A: Chem.* 229 (2005) 77.
- [57] A.M. Rigby, M.V. Frash, *J. Mol. Catal. A: Chem.* 126 (1997) 61.
- [58] J.A. Lercher, K. Seshan, *Curr. Opin. Sol. State Mat. Sci.* 2 (1997) 57.
- [59] S.R. Blaszowski, M.A.C. Nascimento, R.A. van Santen, *J. Phys. Chem.* 100 (1996) 3463.
- [60] M. Guisnet, N.S. Gnep, C. Bearez, F. Chevalier, *Stud. Surf. Sci. Catal.* 5 (1980) 77.
- [61] C. Bearez, F. Avendano, F. Chevalier, M. Guisnet, *Bull. Soc. Chim. Fr.* (1985) 346.
- [62] M.-T. Tran, N.S. Gnep, M. Guisnet, P. Nascimento, *Catal. Lett.* 47 (1997) 57.
- [63] M.-T. Tran, N.S. Gnep, G. Szabo, M. Guisnet, *J. Catal.* 174 (1998) 185.
- [64] F. Chevalier, M. Guisnet, F. Avendano, 9th IberoAmerican Symposium on Catalysis, Lisboa, 1984, p. 1671.
- [65] J. Engelhardt, *J. Catal.* 164 (1996) 449.
- [66] K.B. Fogash, Z. Hong, J.A. Dumesic, *J. Catal.* 173 (1998) 519.
- [67] J. Engelhardt, J. Valyon, *J. Catal.* 181 (1999) 294.
- [68] F. Avendano, PhD Thesis, University of Poitiers, 1984.
- [69] C. Bearez, PhD Thesis, University of Poitiers, 1981.
- [70] M.A. Sanchez-Castillo, N. Agarwal, C. Müller, R.D. Cortright, R.J. Madon, J.A. Dumesic, *J. Catal.* 205 (2002) 67.
- [71] M.-T. Tran, N.S. Gnep, G. Szabo, M. Guisnet, *Appl. Catal. A: Gen.* 171 (1998) 207.
- [72] M. Guisnet, N.S. Gnep, S. Morin, *Microp. Mesop. Mat.* 35–36 (2000) 47.
- [73] M. Guisnet, S. Morin, N.S. Gnep, in: C. Song, J.M. Garces, Y. Sugi (Eds.), *Shape Selective Catalysis*, ACS Symposium Series, vol. 738, ACS, Washington, DC, 1999, p. 334.
- [74] J.A.Z. Pieterse, K. Seshan, J.A. Lercher, *J. Catal.* 195 (2000) 326.
- [75] T.F. Narbeshuber, H. Vinek, J.A. Lercher, *J. Catal.* 57 (1995) 388.
- [76] N.S. Gnep, P. Roger, P. Cartraud, M. Guisnet, B. Juguin, C. Hamon, *C.R. Acad. Sci. Paris, Ser. II*, 1989, p. 1743.
- [77] M. Guisnet, P. Magnoux, *Appl. Catal.* 54 (1989) 1.
- [78] M. Guisnet, P. Magnoux, *Catal. Today* 36 (1997) 477.
- [79] O.A. Anunziata, G.A. Eimer, L.B. Pierella, *Appl. Catal. A: Gen.* 182 (1999) 267.
- [80] D.B. Lukyanov, N.S. Gnep, M. Guisnet, *Ind. Eng. Chem. Res.* 33 (1994) 223.
- [81] D.B. Lukyanov, N.S. Gnep, M. Guisnet, *Ind. Eng. Chem. Res.* 34 (1995) 516.
- [82] N.S. Gnep, J.Y. Doyemet, A.M. Seco, F. Ramôa Ribeiro, M. Guisnet, *Appl. Catal.* 35 (1987) 93.
- [83] N.S. Gnep, J.Y. Doyemet, M. Guisnet, *J. Mol. Catal.* 45 (1988) 281.
- [84] N.Y. Chen, T.Y. Yan, *Ind. Eng. Chem. Process Des. Dev.* 25 (1986) 151.
- [85] J. Weitkamp, Y. Traa, in: G. Ertl, H. Knozinger, J. Weitkamp (Eds.), *Handbook of Heterogeneous Catalysis*, vol. 4, VCH Verlagsgesellschaft mbH, Weinheim, 1997, p. 2039.
- [86] J. Weitkamp, Y. Traa, *Catal. Today* 49 (1999) 193.
- [87] S.I. Hommeltoft, *Appl. Catal. A: Gen.* 221 (2001) 421.
- [88] A. Feller, J.A. Lercher, *Adv. Catal.* 48 (2004) 229.
- [89] A. Corma, A. Martinez, *Catal. Rev.- Sci. Eng.* 35 (1993) 483.
- [90] A. Feller, A. Guzman, I. Zuazo, J.A. Lercher, *J. Catal.* 224 (2004) 80.
- [91] F. Cardona, N.S. Gnep, M. Guisnet, G. Szabo, P. Nascimento, *Appl. Catal. A: Gen.* 128 (1995) 243.
- [92] R. Klingmann, R. Josl, Y. Traa, R. Gläser, J. Weitkamp, *Appl. Catal. A: Gen.* 281 (2005) 215.
- [93] J. Weitkamp, S. Maixner, *Zeolites* 7 (1987) 6.
- [94] M. Stöcker, M. Hostad, T. Rorvik, *Catal. Lett.* 28 (1994) 203.
- [95] C. Flego, I. Kiricsi, W.O. Parker Jr., M.G. Clerici, *Appl. Catal. A: Gen.* 124 (1995) 107.
- [96] J. Pater, F. Cardona, C. Canaff, N.S. Gnep, G. Szabo, M. Guisnet, *Ind. Eng. Chem. Res.* 38 (1999) 3822.
- [97] F.A. Diaz-Mendoza, L. Pernet-Bilano, N. Cardona-Martinez, *Thermochim. Data* 312 (1998) 47.
- [98] G.S. Nivarthi, Y. He, K. Seshan, J.A. Lercher, *J. Catal.* 176 (1998) 47.

- [99] A. Feller, J.O. Barth, A. Guzman, I. Zuazo, J.A. Lercher, *J. Catal.* 220 (2003) 192.
- [100] L.M. Petkovic, D.M. Ginosar, *Appl. Catal. A: Gen.* 275 (2004) 235.
- [101] L. Petkovic, D.M. Ginosar, K.C. Burch, *J. Catal.* 234 (2005) 328.
- [102] C.A. Querini, *Appl. Catal. A: Gen.* 163 (1997) 199.
- [103] C.A. Querini, *Catal. Today* 62 (2000) 135.
- [104] K.P. de Jong, C.M.A. Mesters, D.G. Groot, *Chem. Eng. Sci.* 51 (1996) 2053.
- [105] M.F. Simpson, J. Wey, S. Sundaresan, *Ind. Eng. Chem. Res.* 35 (1996) 3861.
- [106] R. Loenders, P.A. Jacobs, J.A. Martens, *J. Catal.* 176 (1998) 555.
- [107] R. Josl, R. Klinmann, Y. Traa, R. Gläser, J. Weitkamp, *Catal. Commun.* 5 (2004) 239.
- [108] M. Suer, Z. Dardas, Y. Ma, W. Moser, *J. Catal.* 162 (1996) 320.
- [109] L. Vradman, M. Herskowitz, E. Korin, J. Wisniak, *Ind. Eng. Chem. Res.* 40 (2001) 1589.
- [110] D.N. Thompson, D.M. Ginosar, K. Coates, *Fuel Chem. Prepr. ACS* 46 (2001) 422.
- [111] D.M. Ginosar, D.N. Thompson, K. Coates, D.J. Zalewski, R.V. Fox, US Patent 6 579 821 assigned to: Betchel BWXT Idaho, LLC, 2003.
- [112] D.M. Ginosar, D.N. Thompson, K.C. Burch, *Appl. Catal. A: Gen.* 262 (2004) 223.
- [113] D.N. Thompson, D.M. Ginosar, K.C. Burch, *Appl. Catal. A: Gen.* 279 (2005) 109.
- [114] C.-L. Yang, US Patent 3893942 assigned to: Union Carbide Corporation, 1975.
- [115] G. Panattoni, C.A. Querini, *Stud. Surf. Sci. Catal.* 139 (2001).
- [116] M.C. Clark, B. Subramaniam, *Ind. Eng. Chem. Res.* 37 (1998) 1243.
- [117] B. Subramaniam, *Appl. Catal. A: Gen.* 212 (2001) 421.
- [118] B. Subramanian, V. Arunajatesan, C. Lyon, *Stud. Surf. Sci. Catal.* 126 (1999) 63.
- [119] A.S. Chellapa, R.C. Miller, W.J. Thompson, *Appl. Catal. A: Gen.* 209 (2001) 359.
- [120] D.M. Ginosar, D.N. Thompson, K. Coates, D.J. Zalewski, *Ind. Eng. Chem. Res.* 41 (2002) 2864.
- [121] J.A. Johnson, J.A. Weiszmann, G.K. Hilder, H.P. Hall, NPRA Annual Meeting, San Antonio, TX, 1984, AM84/85.
- [122] J.R. Mowry, D.C. Martindale, H.P. Hall, *Arab. J. Sci. Eng.* 10 (1985) 367.
- [123] G.N. Roosen, A. Orioux, J. Andrews, Dewitt's Houston Conference, 1989.
- [124] L. Mank, A. Minkinen, R. Shaddick, *Hydrocarb. Technol. Int.* (1992) 69.
- [125] Z-Forming Process, Mitsubishi Oil Co. Ltd. and Chiyoda Corp., 1994.
- [126] P.B. Weisz, *Adv. Catal.* 13 (1962) 137.
- [127] G.L. Price, V. Kanazirev, K.M. Dooley, V.I. Hart, *J. Catal.* 173 (1998) 17.
- [128] P.P. Notté, *Top. Catal.* 13 (2000) 387.
- [129] C. Bearez, F. Chevalier, M. Guisnet, *React. Kinet. Catal. Lett.* 22 (1983) 405.
- [130] M. Guisnet, G. Perot, in: F.R. Ribeiro, et al. (Eds.), *Zeolites: Science and Technology*, NATO ASI series, vol. 80, 1984.
- [131] M. Guisnet, N.S. Gnep, *Catal. Today* 31 (1996) 275.
- [132] M. Barré, PhD Thesis, University of Poitiers, 1995.
- [133] B. Zheng, W. Hua, Y. Yue, Z. Gao, *J. Catal.* 232 (2005) 143.
- [134] P. Meriaudeau, M. Primet, *J. Mol. Catal.* 61 (1990) 227.
- [135] R.J. Kokes, A.L. Dent, *Adv. Catal.* 22 (1972) 1.
- [136] P. Mériaudeau, C. Naccache, *J. Mol. Catal.* 59 (1990) L31.
- [137] C.R. Bayense, A.J.H.P. van der Pol, J.H.C. van Hooff, *Appl. Catal.* 72 (1991) 81.
- [138] T. Inui, in: T. Inui. (Ed.), series, vol. 44, Elsevier, 1989.
- [139] J. Yao, R. le van Mao, L. Dufresne, *Appl. Catal.* 65 (1990) 175.
- [140] E. Iglesia, J.E. Baumgartner, G.L. Price, *J. Catal.* 134 (1992) 549.
- [141] E. Iglesia, J.E. Baumgartner, G.D. Meitzner, 10th Int. Cong. Catal. New Frontiers in Catalysis, 1992, p. 2353.
- [142] G.D. Meitzner, E. Iglesia, J.E. Baumgartner, E.S. Huang, *J. Catal.* 140 (1993) 209.
- [143] V. Kanazirev, G.L. Price, K.M. Dooley, *J. Chem. Soc. Chem. Commun.* 9 (1990) 712.
- [144] G.L. Price, V. Kanazirev, *J. Catal.* 126 (1990) 267.
- [145] G.L. Price, V. Kanazirev, *J. Mol. Catal.* 66 (1991) 115.
- [146] V. Kanazirev, G.L. Price, K.M. Dooley, in: P.A. Jacobs, et al. (Eds.), *Zeolite Chemistry and Catalysis*, series vol., Elsevier, 1991.
- [147] J.F. Joly, H. Ajot, E. Merlen, F. Raatz, F. Alario, *Appl. Catal. A: Gen.* 79 (1991) 249.
- [148] R. Carli, C.L. Bianchi, R. Giannantonio, V. Ragaini, *J. Mol. Catal.* 83 (1993) 379.
- [149] B.S. Kwak, W.M.H. Sachtler, *J. Catal.* 145 (1994) 456.
- [150] G.J. Buckles, G.J. Hutchings, *Catal. Today* 31 (1996) 233.
- [151] E.G. Derouane, S.B. Abdul Hamid, I.I. Ivanova, N. Blom, P.-E. Hojlund-Nielsen, *J. Mol. Catal.* 86 (1994) 371.
- [152] V.B. Kazansky, I.R. Subbotina, R.A. van Santen, E.J.M. Hensen, *J. Catal.* 233 (2005) 351.
- [153] M.V. Frash, R.A. van Santen, *J. Phys. Chem. A* 104 (2000) 2468.
- [154] M.S. Pereira, A.A.C. Nascimento, *Chem. Phys. Lett.* 406 (2005) 446.
- [155] Y.V. Joshi, K.T. Thomson, *Catal. Today* 105 (2005) 106.
- [156] I. Nowak, J. Quartararo, E.G. Derouane, J.C. Védrine, *Appl. Catal. A: Gen.* 251 (2003) 107.
- [157] S. Kaliaguine, G. Lemay, A. Adnot, S. Burelle, R. Audet, G. Jean, J.A. Sawicki, *Zeolites* 10 (1990) 559.
- [158] K.M. Dooley, C. Chang, G.L. Price, *Appl. Catal. A: Gen.* 84 (1992) 17.
- [159] G. Giannetto, A. Montes, N.S. Gnep, A. Florentino, P. Cartraud, M. Guisnet, *J. Catal.* 145 (1994) 86.
- [160] G. Giannetto, G. Léon, J. Papa, R. Monque, R. Galiasso, Z. Gabelica, *Catal. Lett.* 22 (1993) 381.
- [161] K.M. Dooley, G.L. Price, V.I. Kanazirev, V.I. Hart, *Catal. Today* 31 (1996) 305.
- [162] V. Kanazirev, R. Piffer, H. Förster, *J. Mol. Catal.* 69 (1991) L15.
- [163] N.Y. Chang, W.O. Haag, T.J. Huang, US Patent 4269839, 1981.
- [164] K.H. Steinberg, U. Mroczek, F. Roessner, *Appl. Catal.* 66 (1990) 37.
- [165] W. Reschetilowski, V. Mroczek, K.-H. Steinberg, K.P. Wendlandt, *Appl. Catal.* 78 (1991) 257.
- [166] O.V. Chetina, T.V. Vascina, V. Lunin, *Appl. Catal. A: Gen.* 131 (1995) 7.
- [167] T. Mole, S.R. Anderson, G. Creer, *Appl. Catal.* 17 (1985) 127.
- [168] M.S. Scurrrell, *Appl. Catal.* 41 (1988) 89.
- [169] H. Berndt, G. Lietz, J. Völter, *Appl. Catal.* 146 (1996) 351.
- [170] H. Berndt, G. Lietz, J. Völter, *Appl. Catal.* 146 (1996) 365.
- [171] N. Kumar, L.E. Lindfors, *Catal. Lett.* 38 (1996) 239.
- [172] J.A. Biscardi, G.D. Meitzner, E. Iglesia, *J. Catal.* 179 (1998) 192.
- [173] J.A. Biscardi, E. Iglesia, *J. Catal.* 182 (1999) 117.
- [174] V.B. Kazansky, V. Yu Borovkov, A.L. Serikk, R.A. van Santen, B.G. Anderson, *Catal. Lett.* 66 (2000) 39.
- [175] L.M. Lubango, M. Scurrrell, *Appl. Catal.* 235 (2002) 265.
- [176] C.P. Nicolaidis, N.P. Sincadu, M.S. Scurrrell, *Catal. Today* 71 (2002) 429.
- [177] V.B. Kazansky, E.A. Pidko, *J. Phys. Chem. B* 109 (2005) 2103.
- [178] V.B. Kazansky, I.R. Subbotina, N. Rane, R.A. Van Santen, E.J.M. Hensen, *Phys. Chem. Chem. Phys.* 7 (2005) 3088.
- [179] Y.G. Kolyagin, V.V. Ordomsky, Y.Z. Klimyak, A.I. Rebrov, F. Fajula, I.I. Ivanova, *J. Catal.* 238 (2006) 122.
- [180] R.C.P. Bittencourt, M. Schmal, Y.L. Lam, *Anais. Ass. Bras. Quim.* 40 (1991) 13.
- [181] C.C. Salguero, Y.L. Lam, M. Schmal, *Catal. Lett.* 47 (1997) 143.
- [182] A. Krogh, A. Hagen, T.W. Hansen, C.H. Christensen, I. Schmidt, *Catal. Comm.* 4 (2003) 627.
- [183] F. Solymosi, A. Szoke, *Appl. Catal. A: Gen.* 166 (1998) 225.
- [184] D. Seddon, *Catal. Today* 6 (1998) 351.
- [185] P. Meriaudeau, G. Sapaly, G. Wicker, C. Naccache, *Catal. Lett.* 27 (1994) 143.
- [186] A. Roumégous, PhD Thesis, University of Paris 6, 1978.
- [187] R.A. Asuquo, G. Eder-Mirth, J.A. Lercher, *J. Catal.* 155 (1995) 376.
- [188] R.A. Asuquo, G. Eder-Mirth, K. Seshan, J.A.Z. Pieterse, J.A. Lercher, *J. Catal.* 168 (1997) 292.

- [189] P. Cañizares, A. de Lucas, F. Dorado, D. Pérez, *Appl. Catal. A: Gen.* 190 (2000) 233.
- [190] P. Cañizares, A. de Lucas, F. Dorado, *Appl. Catal. A: Gen.* 196 (2000) 225.
- [191] P. Cañizares, F. Dorado, P. Sanchez-Herrera, *Appl. Catal. A: Gen.* 217 (2001) 69.
- [192] P. Cañizares, A. de Lucas, F. Dorado, *Microp. Mesop. Mat.* 42 (2001) 245.
- [193] F. Dorado, R. Romero, P. Cañizares, *Appl. Catal. A: Gen.* 236 (2002) 235.
- [194] F. Dorado, R. Romero, P. Cañizares, A. Romero, *Appl. Catal. A: Gen.* 274 (2004) 79.
- [195] H. Liu, G.D. Lei, W.M.H. Sachtler, *Appl. Catal. A: Gen.* 137 (1996) 167.
- [196] G. Bellussi, A. Giusti, L. Zanibelli, US Patent 5 336 830 assigned to: Eniricerche S.P.A. and Snamprogetti, 1994.
- [197] G.D. Pirngruber, K. Seshan, J.A. Lercher, *J. Catal.* 190 (2000) 396.
- [198] H. Nagata, T. Igushi, Y. Takyama, M. Kishida, K. Wakabayashi, 11th International Zeolite Conference, Seoul, Korea, 1995, RP120.
- [199] R. Byggningsbacka, N. Kumar, L.-E. Lindfors, *Catal. Lett.* 55 (1998) 173.
- [200] M.M. de Agudelo, T. Romero, J. Guaregua, M. Gonzalez, US Patent 5 416 052 assigned to: The British Petroleum Company, 1995.
- [201] S. Sciré, G. Burgio, C. Crisafelli, S. Minicò, *Appl. Catal. A: Gen.* 274 (2004) 151.
- [202] Ch.-L. O'Young, J.E. Browne, J.F. Matteo, R.A. Sawicki, J. Hazen, US Patent 5 198 597 assigned to: Texaco Inc., 1993.
- [203] G.D. Pirngruber, K. Seshan, J.A. Lercher, *J. Catal.* 190 (2000) 338.
- [204] G.D. Pirngruber, O.P.E. Zinck-Stagno, K. Seshan, J.A. Lercher, *J. Catal.* 190 (2000) 374.
- [205] S.B. Derouane-Abd Hamid, D. Lambert, E.G. Derouane, *Catal. Today* 63 (2000) 237.
- [206] A. Vieira, M.A. Tovar, C. Pfaff, B. Méndez, C.M. López, F.J. Machado, J. Goldwasser, M.M. Ramírez de Agudelo, *J. Catal.* 177 (1998) 60.
- [207] F.J. Machado, C.M. López, Y. Campos, A. Bolívar, S. Yunes, *Appl. Catal. A: Gen.* 226 (2002) 241.
- [208] F. Alvarez, F. Ramôa Ribeiro, G. Perot, C. Thomazon, M. Guisnet, *J. Catal.* 13 (1996) 138.
- [209] M. Guisnet, P. Andy, N.S. Gnep, E. Benazzi, C. Travers, *Oil Gas Sci. Technol.* 54 (1999) 23.
- [210] P. Meriaudeau, A. Thangaraj, J.F. Dutel, C. Naccache, *J. Catal.* 167 (1987) 180.
- [211] S. Sealy, Y. Traa, *Appl. Catal. A: Gen.* 294 (2005) 273.
- [212] S.I. Abasov, F.A. Babayeva, R.R. Zarbaliyev, G.G. Abbasova, D.B. Tagiyev, M.I. Rustamov, *Appl. Catal. A: Gen.* 251 (2003) 267.
- [213] S. Kato, K. Nakagawa, N.-O. Ikenaga, T. Suzuki, *Catal. Lett.* 73 (2001) 175.
- [214] S. Todorova, B.-L. Su, *Catal. Today* 93–95 (2004) 417.
- [215] O.V. Bragin, T.V. Vasina, S.A. Isaev, *Izv. Akad. Nauk USSR, Ser. Khim.* 7 (1987) 1682.
- [216] T.V. Vasina, S.A. Isaev, O.V. Bragin, B.K. Nefedov, US USSR, No. 1426966, 1988.
- [217] S.A. Isaev, T.V. Vasina, O.V. Bragin, *Izv. Akad. Nauk USSR, Ser. Khim.* 10 (1991) 2228.
- [218] I.I. Ivanova, N. Blom, E.G. Derouane, *J. Mol. Catal. A: Chem.* 109 (1996) 157.
- [219] E.G. Derouane, H. He, S.B. Derouane-Abd Hamid, D. Lambert, I. Ivanova, *J. Mol. Catal. A: Chem.* 158 (2000) 5.
- [220] S. Siffert, B.L. Su, *React. Kinet. Catal. Lett.* 68 (1999) 161.
- [221] S. Todorova, B.-L. Su, *J. Mol. Catal. A: Chem.* 201 (2003) 223.
- [222] C. Bigey, B.-L. Su, *J. Mol. Catal. A: Chem.* 209 (2004) 179.